INDEPENDENT COMPONENT ANALYSIS OF EVOKED POTENTIALS TO ESOPHAGEAL STIMULATION

INDEPENDENT COMPONENT ANALYSIS OF EVOKED POTENTIALS TO ESOPHAGEAL STIMULATION

By
WINDY LI JIAN YING, B.ENG

A Thesis Submitted to
the School of Graduate Studies
in Partial Fulfillment of the Requirements
for the Degree
Master of Engineering

McMaster University

Master of Engineering (2001) McMaster University

(Electrical and Computer Engineering) Hamilton, Ontario

TITLE: Independent Component Analysis of Evoked Potentials to Esophageal Stimulation

AUTHOR: Windy Li Jian Ying, B.Eng. (South China University of Technology)

SUPERVISOR: Dr. Markad V. Kamath, Ph.D., P.Eng.

NUMBER OF PAGES: xiv, 77

To my parents Li Fu Tang and Tan Shi Zhen

my brother Li Yin

and my friend Chris

for their support and encouragement

Abstract

Cortical evoked potential to electrical stimulation of the esophagus is a relatively novel modality and is a useful clinical tool. Evoked Potentials (EP) represents the bioelectrical response of the brain elicited by an external sensory stimulation to either an organ or a receptor. Since the physiological study suggests that there are several neuronal sources involved, the EP signal is a mixture of their responses. The traditional way of directly measuring the signal recorded by the electrodes is similar to trying to listen to a group of people speaking at the same time. A lot of information might be lost if we can not pickup the information from each individual. Independent Component Analysis (ICA) is a new technique that can extract the signals according the independence of the sources. It can separate the recorded EP signal into different components given sufficient number of input channels.

In this research we apply ICA to 41 sets of esophageal EP signals recorded from twenty channels in 8 human subjects. We test the reproducibility of the algorithm and compare the components arising from periodic and random stimulation protocol from these subjects. The results show that EPs and their independent components are reproducible. Four pairs of component pairs are found and their scalp distribution maps and activation waveform provide interesting information for further study. Also, ICA isolate and extract a

widely distributed stimulus artifact as a single output component, and remove it from the reconstructed signal . These results demonstrate that ICA could parsimoniously decompose esophageal EP signals into temporally independent, spatially fixed, and physiologically plausible components.

ICA opens a new window to study the esophageal EP signal and provides new information that we were not able to obtain from other signal-processing techniques.

Electrical stimulation (ES) of the esophagus can also be used to study the afferent and efferent pathways of human subjects. In a study of 7 patients with gastroesophageal reflux disease, 9 patients with noncardiac chest pain and 12 controls we found clinically useful information during electrical stimulation of the esophagus. Patients with NCCP had low amplitude cortical EP with increased vagal response during ES when compared to controls. Patients with GERD had high resting sympathetic tone and normal EPs but lower vagal response to ES when compared to normal subjects.

Acknowledgement

I would like to thank my supervisor Dr. Markad V. Kamath for his supervision throughout the course of this work. Without his guidance, support and encouragement, this research would not have been possible.

I am very grateful to Dr.G. Tougas, M.D., Associate Professor of Medicine and to Dr.Adrian Upton, M.D., Professor of Medicine and Director of Neurology in the Medical School for providing facilities to conduct the research reported in this thesis. I acknowledge the financial support of deGroote Foundation to develop the laboratories for conducting evoked potential research.

A number of individuals contributed to my research both directly and indirectly. My discussions with Jeff Fortuna and Derek Schuurman helped me immensely during the algorithm development phase. I also want to thank Kamran Rahbar for verifying my result with other ICA techniques.

I wish to place on record the assistance received from Mr. Glen Shine for his technical support and assistance in data acquisition and Ms.Cindy James who recruited many of the subjects and patients. I want to acknowledge Ms. Tineke Cermak, Ms. Mary Jane Denardis and Ms. Debbie Fitzpatrick for their EEG expertise.

I enjoyed working with Clement Pang, Nesrene Salem, Wendy Wong and Shingo Yuki, my colleagues during graduate study.

Finally, I want to thank my family who nourished my intellectual development with continuous words of encouragement and provided an atmosphere of discovery during my years of study in China and Canada. I also recall my friends who provided a congenial atmosphere during my study at McMaster University.

Contents

List of Figures

List of Tables

List of Acronyms

BSS	Blind source separation
CC	Correlation coefficients
CNS	Central nervous system
CV	Coefficients of variation
EEG	Electroencephalogram
EP	Evoked Potential
ERP	Event-related potentials
GERD	Gastroesophageal reflux disease
GI	Gastro-intestinal
ICA	Independent Component Anaysis
Infomax	Information maximization
NCCP	Noncardiac chest pain
NPCA-RLS	Recursive least-squares algorithm for a nonlinear PCA
p.d.f.	Probability density functions
PCA	Principal Component Analysis

Chapter 1

Introduction

1.1 Background

Evoked Potentials (EP) represent the bioelectrical response of the brain elicited by an external sensory stimulation to either an organ or a receptor. They are also referred to as event-related potentials (ERP), because they are time-locked to a set of identical stimuli (event). Cortical evoked potential to electrical stimulation of the esophagus is a relatively novel modality and is the focus of this thesis. This new modality of stimulation is delivered to the esophagus through a minimally invasive probe and is a useful tool to study diseases that may involve visceral sensory processing. Pathological conditions that may involve visceral sensory inputs include noncardiac chest pain (NCCP), gastroesophageal reflux disease (GERD), diffuse esophageal spasms and nutcracker's esophagus among others [31].

The esophageal EP signal as recorded on the scalp contains three or four peaks and demonstrate a reproducible pattern within and between individuals. Functional

information about the activation of various nuclei within the brain and along the transmission path of the evoked potential signal can be obtained by an analysis of the

latency, amplitude and topographic distribution of the EP waveform. Physiological basis of the EP signal suggests that EP is a summation of potentials arising of different sources, which are created by current fields generated by groups of neurons in the brain.

Much of the research on evoked potentials analyzes the waveform lasting several hundred milliseconds after a stimulus. Independent component analysis (ICA) is a signal processing method that has been developed over the last decade for blind source separation (BSS) and is of value in EP signal analysis. It aims at separating independent sources from a mixed version of component signals without the requirement of knowing how the signals are mixed and what are the constituent signal sources. Since it is difficult to know which sources in the brain produce the response as recorded on the scalp and also because we lack of knowledge about how those sources are mixed when they reach the scalp, ICA is an ideal tool for EP signal analysis. Moreover, decomposing the EP signal with Wavelet or Fourier transformations may impose their mathematical structures on the EP signal. We believe that ICA would enable us to separate naturally occurring components, so that functional information about their transmission can perhaps help us to identify pathological conditions arising out of NCCP and GERD.

Independent component analysis provides a neural network solution for the unmix problem, by making the outputs as statistically independent as possible. Although the neural mechanisms that produce the EP are not fully understood, basic assumptions for

implementing ICA algorithm to the EP signal are generally compatible with the nature of the EP signal. For example, such assumptions include the sources
generating the peaks and valleys in the waveform are independent and the propagation delays of the 'mixing medium' are negligible.

Evoked potential signal recorded with N electrodes can be reconstructed as a sum of N independent components. The output components of ICA can be specified by a fixed linear spatial filter that determines a time course of activation during each stimulus, together with a fixed pattern of strengths at each scalp electrode. ICA obtains these components without trying to specify their location within the brain. In this way, we can simplify the traditional inverse problem of EP by separating the sources and solving a subset of the signal localization problem [20].

ICA has also proved useful in the removal of artifacts from both EEG and EP signals. Besides the finding that EEG can be decomposed into overlapping phenomena, Makeig et al. also show ICA can separate components attributable to artifacts [18]. Jung et al developed the technique to deal with a subgaussian signal, which enables ICA to efficiently separate the line noise and low frequency eye moment artifacts, which have subgaussian distribution [21].

Research reported by Makeig et al [2, 9, 18, 21, 22, 23] is based on auditory or visual EP signals. The usefulness of ICA in understanding origins of different components within the cortical EPs recorded in response to esophageal stimulation has not been explored in literature. Since esophageal EP is generated by a sensory system different from auditory and visual modalities, we believe that analyzing esophageal EP through ICA can help us understand the genesis of this particular modality of EP signal.

Therefore, in this thesis, we implement the ICA algorithm to process cortical EPs to esophageal stimulation, in order to obtain a deeper understanding of how the brain processes signals arising out of the esophagus.

1.2 Objectives

The objectives of this research are as follows:

1. To study components that make up the cortical EP through independent component analysis and study their activation waveform and evaluate its reproducibility and scalp distribution
2. To study the independent components due to periodic and random stimulation as well as the cortical maps arising out of such analysis

1.3 Organization of the thesis

This thesis is organized as follows: In chapter 2, the background information on EEG, and esophageal EPs is provided. The ICA theory and details of EP analysis will be explained in Chapter 3. Chapter 4 will focus on the experimental set up, signal acquisition and the details of implementing ICA. In Chapter 5 we will present the results of our studies. A discussion of the research will follow in Chapter 6. Chapter 7 will summarize the research presented herein. We also propose suggestions for further research.

In summary, ICA is a useful tool for solving traditional blind source unmix problems. Esophageal EP research is a novel but relatively unexplored area. In this context ICA may help us understand the sources that contribute to cortically recorded EPs to esophageal stimulation.

Chapter 2

The Electroencephalogram and Evoked Potentials to Esophageal Stimulation

In this chapter, some background knowledge of EEG will be reviewed. Following a brief introduction, we will examine the physiological basis of EEG and how it is recorded and processed. Details of the signal acquisition and characteristics of evoked potential signals will be presented with particular emphasis on the esophageal EPs.

2.1 Human electroencephalogram (EEG)

The electroencephalogram (EEG) represents the bioelectric activity of the brain as recorded on the scalp. It is obtained by applying an array of surface electrodes to the scalp and amplifying the surface potentials through a set of high gain, high CMRR (common mode rejection ratio, >90db) amplifiers. Dr. Hans Berger first recorded EEG on the scalp in 1929. The EEG quickly became an important clinical tool following discovery of electroencephalographic patterns characteristic of epilepsy [24]. Nowadays, the applications of EEG include an assessment of neurological state in diseases such as

epilepsy, states of altered consciousness in head trauma and coma, anoxia, intoxication and others [25].

2.2 Physiological basis of the EEG

Voltage fluctuations recorded as EEG are summations of the electrical activity of populations of neurons [25]. The EEG record reflects the extracellular currents resulting from postsynaptic membrane depolarizations and hyperpolarizations of pyramidal neurons in cerebral cortex [24]. Each electrical current within the nerve cells produces a surrounding electrical field that decreases in strength.

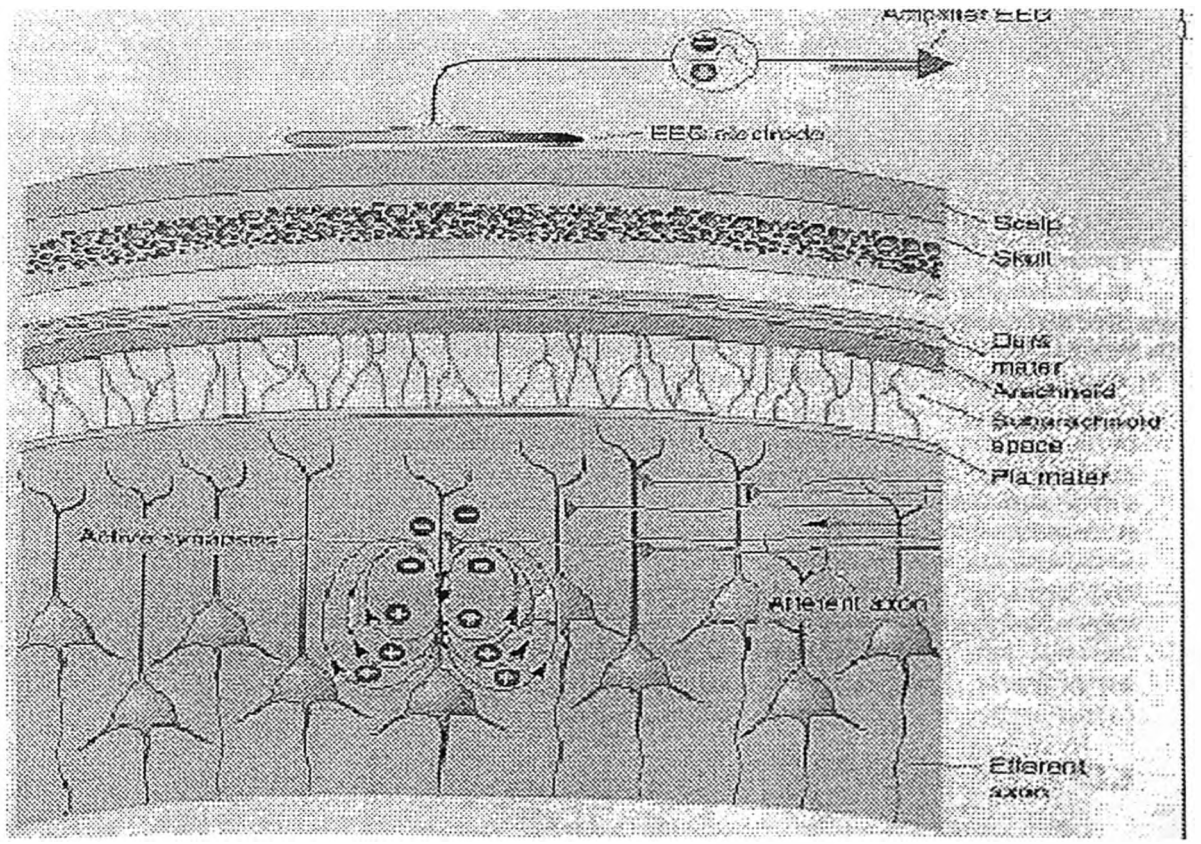

Figure 2.1[26] A schematic of various cortical layers

The current field can be positive or negative. The anatomical position of dipoles within the brain results in the generation of relatively large electrical fields. These electrical fields extend out through the brain, the coverings of the cortex, cerebrospinal fluid surrounding the brain, the skull and the scalp, where they are sensed by EEG electrodes.

2.3 Recording of the EEG Signal

Whereas EEG can be recorded by inserting needle electrodes inside the brain tissue, the non-invasive scalp recording is the one commonly used because of its safety, convenience and noninvasiveness.

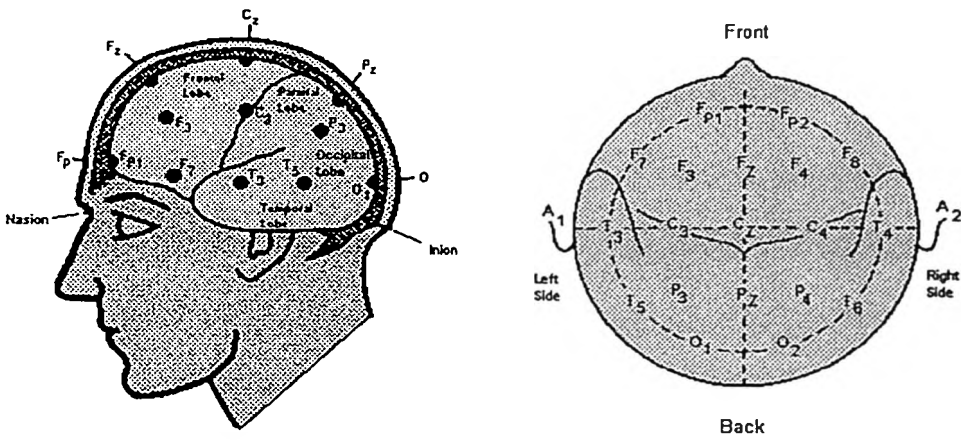

Figure 2.2 International 10-20 system.

The EEG electrode normally consists of a small round cup, made of silver, silver-silverchloride, tin or stainless steel or even gold [26]. It is very important to have an excellent conductivity between scalp and the electrode. (< 5 k Ω). Although there are

many ways of arranging the electrode array on the scalp, the one that is used most often is the international 10-20 system of electrode placement [19]. The international 10-20 system measures the bony landmarks on the skull and determines the location of recording electrodes. A typical set of electrodes (called montage) is shown in Figure 2.2

Two major methods of recording often referred to as bipolar montage and referential montage are in use. Bipolar montage records the EEG signal between any two electrodes, while the referential montage records the difference between an electrode and a common reference located at an isopotential point. In our experiments we use the referential montage with 20 recording electrodes. The isoelectric point is chosen to be mastoids.

2.4 Evoked Potential (Event-Related Potentials)

Evoked Potentials (EPs), also known as Event-Related Potentials (ERPs), are voltages embedded within the electroencephalogram (EEG), that are time-locked to a set of similar repetitive experimental events [17]. These events are usually electrical or mechanical stimuli delivered to a sensory organ or a receptor. EPs signals are reproducible within and between healthy subjects under constraints of similar experimental conditions. Amplitudes and latencies of different peaks within the EP signal are employed to understand functional integrity of the central nervous system (CNS). During the past three decades extensive studies on EPs to electrical, mechanical and other type of stimuli have confirmed their usefulness in clinical medicine[35].

Recently evoked potentials in response to the stimulation gastro-intestinal (GI) tract, especially to the esophagus, have captured the imagination of many researchers [30]. In

this thesis we focus on the signal processing of cortical evoked potentials recorded in response to electrical stimulation of esophagus.

2.5 Stimulation methodologies

Most of the amplifiers and related equipment used for EEG recording can also be used for obtaining EPs. An electrical stimulation device with control on the parameters of stimulation is used for generating the stimulus delivered to the sensory organ, i.e. the esophagus, in our laboratory.

Besides periodical stimulation, one can explore the effects of the random stimulation. Typically, the random stimulation trigger can be obtained by a pseudo-random number generator. This type of stimulation has certain advantages over the periodic stimuli. It has been suggested that the uncertainty of when the random stimulus occurs will diminish the process of habituation that occurs with periodic stimuli [29]. Furthermore, the random stimuli have favorable properties related to suppressing some steady state components of EEG, such as the alpha rhythm. However, the variation of the EP latency and amplitude in response to random stimulation is greater, and may cause some loss of sharpness of peaks within the EP waveform.

2.6 Computation of EP signal through averaging

Averaging is a common processing method for obtaining the EP signal from the background EEG. The basic premise of averaging is that the repeated presentation of an identical stimulus will lead to essentially the same EP each time. The background EEG activity (which is unrelated to stimulus and is considered to be noise) averages out to

zero. It has been shown that the averaging of the EEG can improve the signal-to-noise ratio (SNR) of EP signal by square root of the number of responses that are averaged [27]. However, in practice, merely increasing the number of stimuli need not enhance the SNR, because extraneous factors such as attention and habituation may influence the amplitude and latency of the responses.

2.7 Inverse problem

A major focus of EP research has been, the so-called inverse problem, which aims at localizing the sources that generate the known potential distribution on the scalp [20]. Many models and techniques including dipole localization and cortical projection methods have been proposed. Most of these procedures try to solve source separation and source identification issues all at once, which makes the solution a complex one. It has been suggested that independent component analysis (ICA), an innovative method that uniquely deals with the mathematical source separation of the EP signals, may serve as an alternative useful research tool in the place of classic inverse problem. We will discuss independent component analysis in detail in Chapter 3.

2.8 Esophageal Evoked Potentials

Based on the sensory system being stimulated, one can record different kinds of evoked potentials [34]. Somatosensory EP, for instance, is the response to the stimulus applied to the skin or a sensory nerve. Similarly, there are auditory EPs and visual EPs, which are elicited by means of stimuli delivered to the auditory system and visual system

respectively. Compared to these EPs, the esophageal EP is a relatively new modality and is receiving increasing attention lately. Esophageal EP is especially helpful in studying patients with functional gastrointestinal disorders such as noncardiac chest pain, gastroesophageal reflux, diffuse esophageal spasms and nutcracker esophagus [30]. A further advantage of esophageal stimulation is that it is minimally invasive and causes discomfort only during insertion of the esophageal tube. With esophageal EPs, we may gain new insights into diseases that involve abnormal sensory processing, inflammatory bowel disease (IBD), chronic abdominal pain and chronic inflammatory bowel disorder [30, 31,32, 33].

In practice, the esophageal EP are cerebral evoked potentials that can be elicited by esophageal stimulation of two modalities, either through mechanical or through electrical stimuli. For mechanical stimulation, a balloon is placed within the esophagus and is inflated periodically with a pump. Alternatively, short electrical pulses have been the preferred form of stimulation, because of their specificity. These two methods have different protocols and naturally the resulting EP waveforms are not identical. In this thesis, we focus on the electrical stimulation, which is more convenience to implement.
The esophageal EP waveform to electrical stimulation shows a characteristic triphasic pattern. There are three to four peaks above and below the isopotential line [30].

It has been suggested that peaks in the esophageal EP signal contain important information about the synaptic activity and the functional integrity of the transmission pathways [34]. For example, the latency of the first esophageal EP peak, which is about 76.4±9.3ms, is determined by the type of the afferent nerve fibers that are involved.

Since different fibers have different conduction velocities. One can identify that 'C' fibers are involved [33].

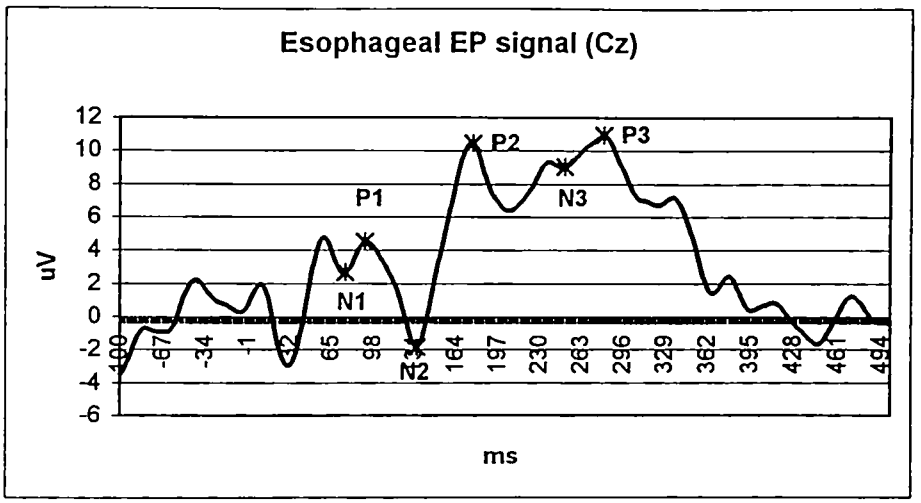

Figure 2.3 Cortical evoked potential to electrical stimulation of the esophagus

It has also been shown that the amplitude of the principal peaks (N1-P1, N2-P2) demonstrate a dose response pattern for intensities varying from 5-25 mA in healthy controls. Similarly the stimulus frequency has an important effect on these peaks [32]. Hollerbach et al. have demonstrated that when stimulated at frequencies varying from 0.1-1 Hz, the principal peaks of the esophageal of EPs reach a maximum at 17.2±1.7 μV. So by analyzing the waveform of esophageal EPs, we can gain useful information regarding the physiology of the transmission pathways. It is believed that such knowledge will eventually provide a better understanding of the origin of the signal for the clinical diagnosis.

In summary, this chapter has presented a review of EEG signal generation and EP signal in response to esophageal electrical stimulation.

Chapter 3

Independent component Analysis

In this chapter mathematical formulation of Independent Component Analysis (ICA) will be presented and will be followed by an algorithm for performing ICA. We will present reasons why ICA is a good analytical tool for an analysis of Evoked Potential (EP) signals.

3.1 What is ICA?

3.1.1 General description

Independent Component Analysis is a novel signal-processing method developed to solve unmix problems. Briefly, ICA is a linear transform of the multivariate input data, which is designed to make the output vectors as statistically independent as possible. Initial ideas for ICA came from blind source separation (BSS) and information theory. The goal of blind source separation is to extract independent sources from a signal given by a series of sensor observations, which are linear mixtures of independent sources. The term "blind source" indicates that both source signals and the way they are mixed is not known *apriori*. ICA is a convenient method to solve BSS. Stated another way, ICA is a

procedure to find a linear coordinate system such that the signals are as independent from each other as possible [2]. In contrast to Principal Component Analysis (PCA), ICA not only decorrelates the signals(2^{nd} order statistics) but also reduces higher order statistical dependencies.

3.1.2 Definition of ICA problem

The objective of independent component analysis is to recover source signals after they were linearly mixed. For example, let us denote the **N** dimensional source signals as **s**, where $s=\{s_1(t), \ldots, s_N(t)\}$. All source signals have zero mean and are statistically independent. Assuming a zero-mean signal model essentially simplifies the algorithm development. If the data is non-zero, one can subtract the sample mean to meet this requirement. The linear mixing can be represented by a matrix **A** . After the mixing, the observed signal is denoted by **x**, where $\mathbf{x} = \{x_1(t), \ldots, x_N(t)\} = \mathbf{AS}$. We are not given information about the signal and how it is mixed, and therefore **S** and **A** are unknown in this problem, Mathematically stated, the goal is to find an inverse transform **W**, such that, given the observed signal **x**, an output **u** can be obtained from the equation

$$\mathbf{u} = \mathbf{Wx} \qquad (3.1.2.1)$$

Output **u** should contain the same components as **s**, although the component order is not necessarily the same. What ICA attempts to do is to minimize the redundancy between the outputs.

Before presenting the ICA estimation, we will examine some basic concepts that help us formulate the ICA algorithm.

3.2 Basic concepts of statistical signal processing and information theory

3.2.1 Independence

In signal processing, we often encounter the term "statistically independent". What does it imply? Consider a simple case of two scalar-valued random variables y_1 and y_2. When they are said to be independent, the information regarding y_1 does not provide any information about y_2, and vice versa.[37] This property can be defined by probability densities. Denote $p_1(y_1)$ and $p_2(y_2)$ as the marginal probability density functions (p.d.f.) of y_1 and y_2 respectively, and $p(y_1, y_2)$ as the joint p.d.f. of these two random vectors. Then

$$p_1(y_1) = \int p(y_1, y_2)\, dy_2 \qquad (3.2.1.1)$$

Then y_1 and y_2 is statistically independent if and only if the joint p.d.f. is factorizable into their marginal p.d.f.. This implies

$$p(y_1, y_2) = p_1(y_1)\, p_2(y_2) \qquad (3.2.1.2)$$

Extending this case to the general situation for any number **n** of random variables, equation 3.2.1.2 becomes

$$p(y_1, y_2 \ldots y_n) = \prod_{i=1}^{n} p_i(y_i) \qquad (3.2.1.3)$$

A very important property of independent random variables can be derived from this definition. Given any two functions, g_1 and g_2, the following equation is always true:

$$E\{ g_1(y_1), g_2(y_2)\} = E\{ g_1(y_1) \} E\{ g_2(y_2)\} \qquad (3.2.1.4)$$

This is proved as follows:

$$E\{ g_1(y_1) , g_2(y_2)\} = \iint g_1(y_1)\, g_2(y_2)\, p(y_1, y_2)\, dy_1\, dy_2$$

$$= \iint g_1(y_1)\, p_1(y_1)\, g_2(y_2)\, p(y_2)\, dy_1\, dy_2$$

$$= \int g_1(y_1)\, p_1(y_1)\, dy_1 \int g_2(y_2)\, p(y_2)\, dy_2$$

$$= E\{ g_1(y_1) \} E\{ g_2(y_2)\} \qquad (3.2.1.5)$$

A weaker form of Independence is uncorrelatedness [40]. For example, we can say two random variables y_1 and y_2 are uncorrelated, when their covariance is zero, which is :

$$E\{ y_1 , y_2\} - E\{ y_1 \} E\{ y_2\} = 0 \qquad (3.2.1.6)$$

This equation is valid when we choose $g_1(y_1) = y_1$ and $g_2(y_2) = y_2$ for equation (3.2.1.4).

However, Independence is much stricter condition than uncorrelatedness, which is imperative when we compare the equation (3.2.1.6) with (3.2.1.4). The special case where these two conditions are equivalent is when the y_1 and y_2 have a joint Gaussian distribution [4]. And because of this special case, ICA is not interesting for Gaussian variables [37].

3.2.2 Information theory basis for ICA

3.2.2.1 Entropy and Negentropy

Entropy is one of the basic concepts we will use often while discussing ICA. Its definition is as follows:

Denote **Y** as a discrete random variable, and a_i are the possible values of **Y**, Then the Entropy **H(Y)** is given as:

$$\mathbf{H(Y)} = -\sum_i \mathbf{P(Y=}a_i\mathbf{)log\ P(Y=}a_i\mathbf{)} \qquad (3.2.2.1)$$

When generalized for the case of continuous valued random variable **y**, it is called differential entropy:

$$\mathbf{H(y)} = -\int \mathbf{p(y)log\ p(y)dy} \qquad (3.2.2.2)$$

It is because a Gaussian variable has the largest entropy among all random variables of equal variance, entropy can be used to assess nongaussianity [47,48]. For this purpose, there is a slightly modified version of the differential entropy, called negentropy **J**, which is zero for a Gaussian variable and is always nonnegative.

$$\mathbf{J(y) = H(ygauss)- H(y)} \qquad (3.2.2.3)$$

Here 'ygauss' denotes the Gaussian random variable with the same covariance matrix as **y**. Since negentropy is an optimal estimator of nongaussianity, maximizing it can be an approach for solving the ICA problem. Computing negentropy is rather difficult, because it requires an estimation of the p.d.f. of the random variable.

3.2.2.2 Mutual Information

The mutual information can be used as a measure of independence. Based on the entropy concepts, we can define the mutual information *I*, between n random variables $\mathbf{y}_i$ as follows, where i=1..n

$$I(\mathbf{y_i\ \ldots y_n}) = \sum_{i=1}^{n} \mathbf{H(y_i)} - \mathbf{H(y)} \qquad (3.2.2.4)$$

This definition is equivalent to the Kullback-Leibler (KL) divergence [37], which describes the mutual information with their joint density p(y) and the product of the marginal densities

$$I(y) = \int p(y) \log \frac{p(y)}{\prod_{i=1}^{n} p_i(y_i)} dy \qquad (3.2.2.5)$$

I(y) is always nonnegative and it has a useful property that is important for ICA: *It is zero if the variables are independent.* This is because, when y_i are statistically independent, p(y) can be factorized according to equation (3.2.1.4)

$$p(y) = \prod_{i=1}^{n} p_i(y_i)$$

When we substitute the equation above into equation (3.2.2.5), mutual information becomes zero.

An important property of KL divergence we can consider is: It is invariant under an invertible transformation. This is one of the key ideas that helped develop the infomax solution of ICA.

The mutual information takes into account the whole dependency structure of the variables [37] , and gives a very direct criteria for ICA development. However, it cannot be directly implemented because equation (3.2.2.5) is very difficult to minimize.

3.2.3 Statistical basis of ICA

Independence involves higher-order statistical information, which is often described by cumulants and moments. Among them, the 4^{th} order cumulants, which is also called kurtosis, is a key parameter for some ICA estimation [2].

Moments are discrete parameters that can be used to describe the p.d.f. of a random variable. If we denote **x** as the random variable, the $\mathbf{n}^{th}$-order moment $\mu_x(n)$ is as follow:

$$\mu_x(n) = \mathbf{E}\{x^n\} = \int_{-\infty}^{+\infty} x^n \, p(x)dx \qquad (3.2.3.1)$$

According to (3.2.3.1), the first-order moment is the mean value of x. Normally, we use central moments because it describes the manner in which the distributions is spread about its mean value. Let us denote the mean for **x** as $\mathbf{m_x}$, then we can calculate the $\mathbf{n}^{th}$-order central moments $\mathbf{m_x}(n)$ from the equation(3.2.3.2)

$$\mathbf{m_x(n) = E\{(x- m_x)^n\}} \qquad (3.2.3.2)$$

For example, the second-order central moment is the variance, which is

$$\mathbf{Variance = E\{(x- m_x)^2\}}$$

Cumulants characterize the random variables as function of mean and moments. They can be computed from the central moments. Our discussion will only involve up to the 4^{th} order. They are defined as:

$$\mathbf{c_x\,(1) = m_x\,(1)}$$

$$\mathbf{c_x\,(2) = m_x\,(2)}$$

$$\mathbf{c_x\,(3) = m_x\,(3)}$$

$$\mathbf{c_x\,(4) = m_x\,(4)- 3m_x^{\,2}\,(2)} \qquad (3.2.3.3)$$

The first three cumulants are equal to their same order center moments. The absolute value of forth-order cumulant (kurtosis), can be taken as a measure of the nongaussianity. Because a zero-mean Gaussian distribution random variables can be completely described by the first and second order statistic, its kurtosis is equal to zero. On the other hand, almost all the random variables that have non-Gaussian distribution have non-zero kurtosis [38]. Based on the sign of kurtosis, we can state if a random variable is subgaussian or supergaussian. Random variables that have a negative kurtosis are called subgaussian and those with positive kurtosis are called supergaussian [39].

3.2.4 Distribution requirements for ICA

The typical supergaussian distribution is more "spiky" and has a heavier tail compared to the Gaussian distribution. Laplace distribution is a typical example of supergaussian distribution [38], which is shown in Figure 3.1. On the other hand the subgaussian distribution is rather "flat", i.e. the uniform distribution [2]

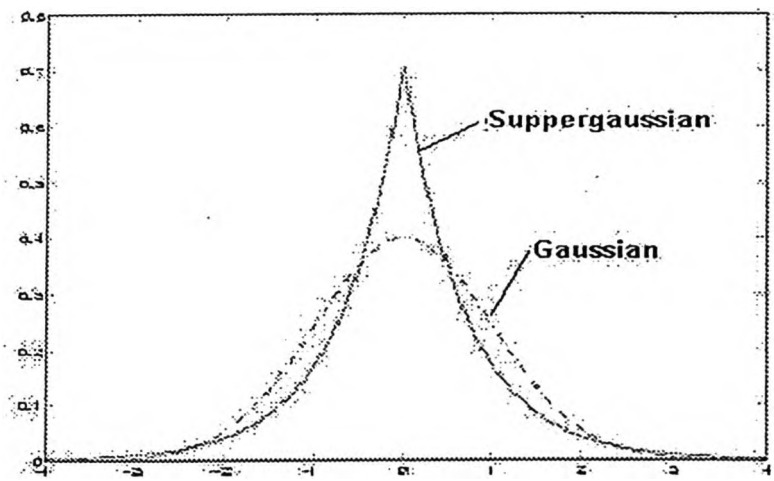

Figure 3.1 Probability Density function for supergaussian and Gaussian distribution.

Since ICA algorithm are based on higher order statistical information, it follows that ICA will not separate a mixture of Gaussians. So the ICA is constructed for nongaussian variables only [37]. This can be illustrated by an example given as following:

Let's assume two sources, s_1 and s_2, have Gaussian probability density distribution. After being mixed by an orthogonal matrix **A**, the observed variable x_1 and x_2 are Gaussian, uncorrelated and have unit variance. Their joint density is

$$p(x_1, x_2) = \frac{1}{2\pi} \exp(-(x_1^2 + x_2^2)/2) \qquad (3.2.4.1)$$

When the density distribution in equation (3.2.4.1) is plotted with x_1 and x_2 as axes, we get a completely symmetric density function, which gives no information about the directions of the columns for estimating the mixing matrix **A** [40]. Therefore, we cannot find an inverse matrix **W** for it. Moreover, it can be proved that the distribution of any orthogonal transformation of the Gaussian has exactly the same distribution [40].

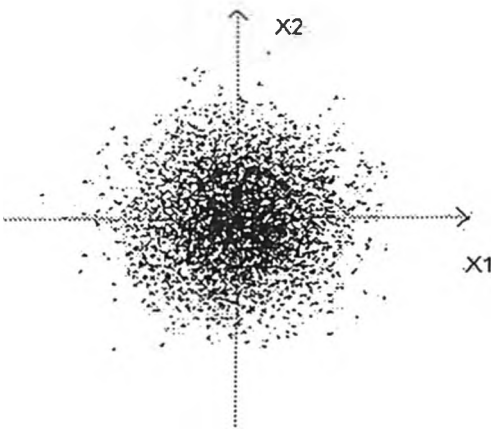

Figure 3.2 The joint distribution of the observed mixtures x_1 and x_2

3.3 Infomax Algorithm for Independent Component Analysis

There are several methods to perform Independent Component Analysis derived from different theoretical backgrounds. It was shown that although they are developed from different principles and not strictly equivalent, they can be unified based on the information theory [37,40,46]. For example, the Maximum Likelihood Estimation (MLE) approach to ICA was proved to be equivalent to the principle of the infomax approach derived by Bell and Sejnowski [49]. Also, the algorithm based on nonlinear PCA criterion can be related to the maximum likelihood estimation [50]. Many cumulant-based algorithm can be reinterpreted as approximation of minimizing the mutual information [37].

When comparing these different algorithms, they all have promising theoretical performance. However, when applied to real data, the accuracy of these algorithm is difficult to ascertain and compare because there are no predetermined solutions for data which have completely unknown sources. The infomax approach has been applied to biomedical signals for many years and has proven to be useful in evoked potential signal analysis. For this reason, we chose infomax algorithm for the current problem. We will discuss ICA solution based on Infomax below.

3.3.1 Information Maximization

Direct minimization of the mutual information equation (3.2.2.5) is a complex task [1]. Therefore, Bell and Sejnowski derived a solution for ICA based on Nadal and

Parga's research. It has been shown that for low-noise data, the maximum of the mutual information between the inputs **x** and the outputs **y** of a neural processor implies that the output distributions can be decomposed into its factors [11]. In other words, maximization of information transfer in a nonlinear neural network, leads to a minimization the mutual information among the outputs, when the optimization is performed over both synaptic weights and nonlinear transfer function [2]. Bell and Sejnowski showed that maximization the joint entropy **H(y)** of the output of a neural processor will approximately minimize the mutual information among the output components [46] .

Denote $\mathbf{g(u_i)}$ as an invertible monotonic nonlineartiy, then $\mathbf{y_i = g(u_i)}$. The joint entropy **H(y)** equation can be derived from equation (3.2.2.4) as follows

$$\mathbf{H(y)} = \sum_{i=1}^{n} \mathbf{H(y_i)} \quad - I(\mathbf{y_i} \ \ldots \mathbf{y_n}) \tag{3.3.1.1}$$

Maximizing the joint entropy **H(y)**, implies that we are maximizing the marginal entropies and minimizing the mutual information. Since outputs $\mathbf{y_i}$ are amplitude-bounded random variables, the marginal entropies are maximum for a uniform distribution of $\mathbf{y_i}$ [46]. And because $I(\mathbf{y_i} \ \ldots \mathbf{y_n})$ is always nonnegative, it will decrease with a maximization of the joint entropy. If $\mathbf{y_i}$ is statistically independent ,

$I(\mathbf{y_i} \ \ldots \mathbf{y_n})=\mathbf{0}$. Equation (3.3.1.1) becomes

$$\mathbf{H(y)} = \sum_{i=1}^{n} \mathbf{H(y_i)} \tag{3.3.1.2}$$

Therefore when maximum joint entropy is achieved, it implies the independence of $\mathbf{y_i}$. As mentioned in section 3.2.2.2, KL divergence is invariant under an invertible transform, thus the nonlinearity **g** will not change the independence of the variables. So

when $I(y_i \ldots y_n)=0$, the mutual information before the nonlinearity $I(u_i \ldots u_n)$ must be zero too, which means u_i are independent. Thus, a solution for ICA problem can be achieved.

There is a constraint in choosing the nonlinear function g, because the derivative of it works as an approximation of the source density in this algorithm. The marginal entropy $H(y_i)$ in equation (3.3.1.1) is given by:

$$H(y_i) = -E\{\log p(y_i)\} \qquad (3.3.1.3)$$

The nonlinear mapping between the output density $p(y_i)$ and sources estimate density $p(u_i)$ can be described by the absolute value of the derivative with respect to u_i [2]

$$p(y_i) = p(u_i)/|(\partial y_i / \partial u_i)| \qquad (3.3.1.4)$$

Which can be substituted in equation (3.3.1.3) and giving

$$H(y_i) = -E\{\log (p(u_i)/|(\partial y_i / \partial u_i)|)\} = E\{\log (|g'(u_i)| / p(u_i))\} \qquad (3.3.1.5)$$

Then the mutual information $I(u)$ related to the joint entropy, $H(y) = H(g(u))$, of the outputs passed through function g can be represent as follows:

$$I(u) = -H(g(u)) + E\left[\sum_i \log \frac{|g'(u_i)|}{p(u_i)}\right] \qquad (3.3.1.6)$$

Thus, if the absolute values of the slopes of the functions $g(u)$, are the same as the independent component p.d.f's, $p(u_i)$, the Infomax criteria discussed above is achieved. Equation (3.3.1.6) also gives the reason of why $|g'(u_i)|$ should be an approximation of $p(u_i)$: if the $|g'(u_i)|$ and the $p(u_i)$ doesn't match, the maximum of $H(y)$ may be achieved without $I(y)$ being zero. The algorithm still works in the cases like this, because although unproven, the robustness conjecture states any supergaussian prior will suffice to extract supergaussian independent components and any subgaussian prior will suffice

to extract subgaussian independent components [54]. This conjecture leads to the generally successful of extended ICA algorithms, which switch the component priors between supergaussian and subgaussian functions [9]. In practices, as the robustness principle suggests, this switching may be all the estimation needed to obtain a correct solution [54]. Bell and Sejnowski had performed a comparison between typical functions of **g** and their research demonstrates that logistic sigmoid $\mathbf{y=(1+e^{-u})^{-1}}$ or the hyperbolic tangent **y= tanh (u)** is flexible enough to sufficiently approximate the EEG source density [51].

3.3.2 Stochastic gradient learning rule

In order to process infomax, we need a nonlinear transfer function **g(u).** Now we can write equation (3.1.2 .1) as the follows:

$$\mathbf{y = g(u) = g(Wx)} \qquad (3.3.2.1)$$

The relation between the output and input probability distributions in equation (3.3.2.1) is described by the following equation [12]:

$$\mathbf{p(y) = p(x)/|}J| \qquad (3.3.2.2)$$

where J is the determinant of the Jacobian matrix $J=\det([\ \partial y_i / \partial x_j\ ]_{ij})$, and $|J|$ denotes its absolute value.

Substituting equation (3.3.2.2) in the entropy definition equation (3.2.2.2)

$$\mathbf{H(y)} = -\mathbf{E}\ [\log \mathbf{p(y)}] = -\int \mathbf{p(y)} \log \mathbf{p(y)} dy$$

We can get

$$\mathbf{H(y) = E}\ [\log |J|] + \mathbf{H(x)} \qquad (3.3.2.3)$$

Since the input entropy **H(x)** is not affected by the change of **W**, the **H(x)** can be ignored when we consider the learning rule for **W** [1].

We now can derive the learning rule for **W** with entropy

$$\partial \mathbf{H(y)} / \partial \mathbf{W} = \mathbf{E}[\partial(\log |J|)/\partial \mathbf{W}] \qquad (3.3.2.5)$$

where $\log |J|$ is given by

$$\log |J| = \log \det \mathbf{W} + \sum_{i=1}^{N} \log |y_i'| \qquad (3.3.2.6)$$

Combining equation (3.3.2.5) and (3.3.2.6), the learning rule for **W** can be presented:

$$\Delta \mathbf{W} \propto \partial(\log |J|)/\partial \mathbf{W} = \mathbf{W}^{-T} + \Phi(\mathbf{u})\mathbf{x}^{T} \qquad (3.3.2.7)$$

Where $[]^{-T}$ denotes the inverse transpose. $\Phi(\mathbf{u})$ is a vector function, which includes the following elements

$$\phi(u_i) = \partial y_i' / \partial y_i = \partial (\log | y_i' |) / \partial u_i \qquad (3.3.2.8)$$

$\phi(u_i)$ depends on the nonlinear function **g** in equation (3.3.2.2). As discussed in section 3.3.1, the **g** is a nonlineartiy which is required not only to be invertible and monotonic but also be able to approximate the source density [2].

The equation (3.3.2.7) is the stochastic gradient learning rule for Infomax ICA algorithm [13]. A pictorial representation of the infomax ICA algorithm is given in Figure 3.3.

3.3.3 Natural gradient rule

In 1996, Amari et al. proposed a procedure to simplify the stochastic-gradient learning rule to the natural gradient rule [14]. The entropy gradient in equation (3.3.2.7)

was multiplied by $\mathbf{W}^T\mathbf{W}$. By doing this, we can avoid performing inversion of $\mathbf{W}$ at every learning step. The learning rule then becomes

$$\Delta \mathbf{W} \propto (\partial(\log |J|)/\partial \mathbf{W})\, \mathbf{W}^T \mathbf{W} = \mathbf{W}\,(\mathbf{I} + \Phi(\mathbf{u})\mathbf{u}^T) \qquad (3.3.3.1)$$

Although equation (3.3.3.1) is not exactly same as equation (3.3.2.7), it has been shown that they yield similar results [15]. Since it is easier to implement equation (3.3.3.1) and has been shown that can speed up the convergence , it is generally used in practice.

3.3.4 Extended Infomax

The original infomax derived by Bell and Sejnowski is suitable for supergaussian sources but doesn't work well for the subgaussian sources [9]. In 1998, Lee et al derived the extended infomax algorithm to handle both subgaussian and supergaussian sources [2].

The supergaussian signal has positive kurtosis, while the subgaussian signal has negative kurtosis. So to estimate the kurtosis of $\mathbf{p_i}(\mathbf{u_i})$, we can switch the term $\phi_i(\mathbf{u_i})$ in equation (3.3.3.1) depending upon the type of the signal.

Based on the Girolami's scheme, we can chose different $\Phi(\mathbf{u})$ for subgaussian and subgaussian sources

$$\begin{cases} \Phi(\mathbf{u}) = \mathbf{u} - \tanh(\mathbf{u}) & \textbf{(subgaussian)} \\ \Phi(\mathbf{u}) = \mathbf{u} + \tanh(\mathbf{u}) & \textbf{(supergaussian)} \end{cases} \qquad (3.3.4.1)$$

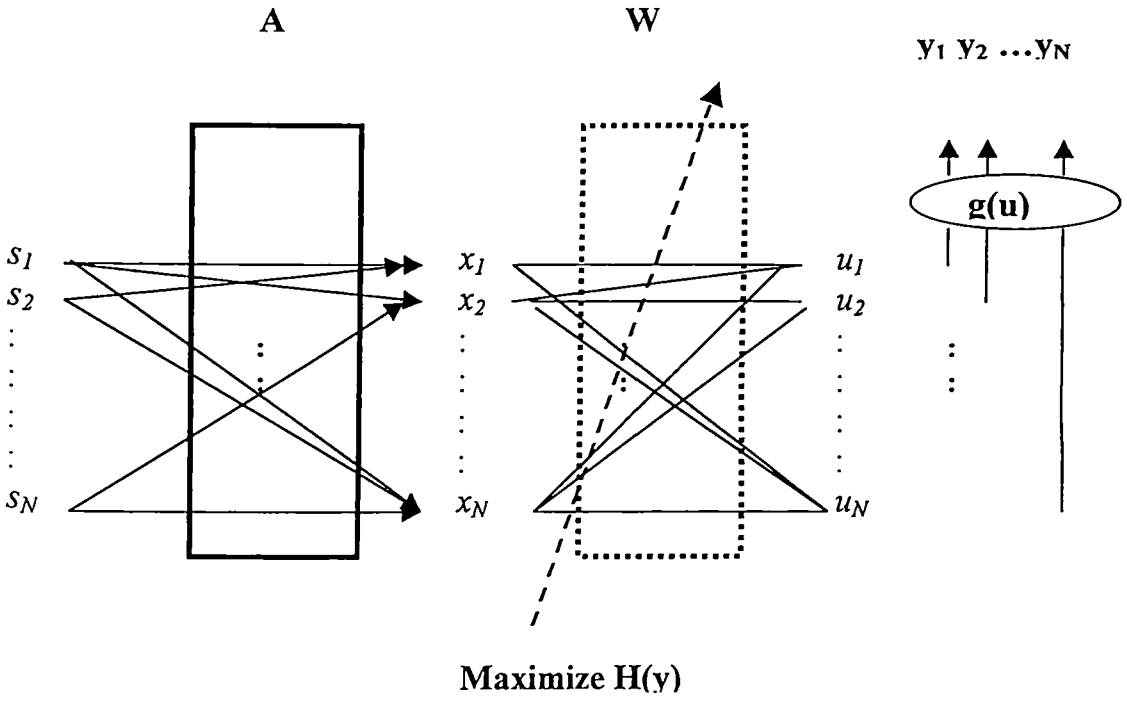

Figure 3.3. The mixing and unmixing model. Independent signal sources **s** become mixed by matrix **A**. The observed signals are **x**. The goal is to learn **W** that inverts the mixing matrix **A** and **u** are the estimates of the recovered sources. The infomax approach is one way to find the unmixing system **W**. It requires a nonlinear transfer function **g(u)** [2]

Substitute equation set (3.3.41) into the natural learning rule, we can obtain the learning rule for subgaussian sources [16]:

$$\Delta W \propto W (I + \tanh(u). u^T - u u^T) \quad (3.3.4.2)$$

And for supergaussian sources learning rule is

$$\Delta W \propto W (I - \tanh(u). u^T - u u^T) \quad (3.3.4.3)$$

Combining equation (3.3.4.2) and equation (3.3.4.3) the extended infomax learning rule as follows:

$$\Delta W \propto W (I - K \tanh(u). u^T - u u^T) \quad (3.3.4.4)$$

For K, $\begin{cases} k_i = 1 & \text{(supergaussian)} \\ k_i = -1 & \text{(subgaussian)} \end{cases}$

In equation (3.3.4.4), k_i is the sign of kurtosis , it can be estimated by the follow equation: [2]

$$k_i = \text{sign}(E\{\text{sech}^2 (u_i)\} E\{ (u_i^2)\} - E\{ \tanh(u_i). u_i \}) \quad (3.3.4.5)$$

The extended infomax provides a practical method to handle both supergaussian and subgaussian sources.

ICA has been successfully used in many signal-processing areas, such as image processing, speech enhancement, telecommunications, and medical signal processing. After Makeig et al [18]. first applied ICA to analyze the EEG data in 1996, ICA is fast becoming an important tool for biomedical signal processing.

3.4 ICA in EEG Analysis

3.4.1 Preprocessing tool for source localization

Many EP studies employ the peak and latency measurement to develop some clinical diagnostic criteria. EPs are not easily decomposed into functionally distinct components, since the time course and scalp projections of those components generally overlap [1]. Research conducted by Makeig et al. on visual evoked response shows that ICA is a very strong candidate for decomposing multiple overlapping components [21]

From Chapter 2, we note that the neural mechanisms that produce EP are not completely known. Anatomical and physiological studies have suggested that sensory perception and processing occur in multiple cortical areas. The interaction of the activity in neuronal fibers connecting cortical areas does not necessarily produce the macroscopic field visible on the scalp [18]. At each stage of EP signal transmission within the brain, potentials are generated by one or more sets of neurons. However, scalp distributions of such potentials may overlap in time and space. This causes the EP topography to shift continuously making it very difficult to identify sources which are spatially fixed. However, in the present context, the inverse problem, which attempts to localize the sources that generated the observed potential distribution on scalp, is a major issue in EEG signal analysis. Therefore, solving the source separation and the source localization problem concomitantly makes the problem a hard one indeed.

In this instance, ICA may specify what temporally independent activations result in the observed potentials (EPs) on the scalp. However, ICA does not indicate where

within the brain these activations arise. *Makeig et al. have shown that ICA can be used to separate the problem of EEG source identification from the problem of localization* [52].

3.4.2 Artifact removal

Since it has been shown that ICA is an efficient tool for separating different signal sources, it has been successfully used in EEG artifact removal [21]. The EEG signal often contains different types of noise which can not be easily removed by other techniques [17]. Since sources of such noise may be different from normal EEG signal generators, ICA can separate such noise by diverting them into separate components. One can then retrieve the uncorrupted EEG by reconstructing the signal without those noisy components. Jung et al. have demonstrated EEG artificial removal using extended infomax ICA in 1997 [2]. The artifacts, such as the blinks, muscle noise, cardiac noise, can be successfully separated.

3.4.3 Validity of ICA Assumptions for EP signal Processing

Following assumptions have to be made when applying ICA analysis to EEG.

1. The sources are statistically independent.
2. The propagation delays of the 'mixing medium' are negligible.
3. Statistical distributions of the component activation values are not Gaussian.
4. The number of independent signal sources is the same as the number of sensors [18].

We will outline below arguments that favor application of ICA to EEG and related signals.

The first assumption is a very general one for modeling the complexity of EEG dynamics [17] and is likely to be valid as generators are anatomically distinct.

Since the volume conduction in brain tissue is instantaneous, and therefore the second assumption is reasonable in practical.

In practice, although some observed EEG signal do appear to be Gaussian, it doesn't imply that their sources are gaussian. Also the central limit theorem suggests that a mixture of nongaussian components may appear Gaussian. Researches of Lee et al shows that the EEG signal contains a number of subgaussian components such as some low frequency activity and the line noise, sensor noise [2]. Therefore the assumption 3 is proven can be satisfied in EEG or EP signals study.

In the case of EEG, assumption 4 implies that if we collect EEG from N electrodes, we can separate only N sources through ICA. This assumption is not easy to satisfy, because we do not know how many source within the brain contributed to the mixed observed cortical signal we collect. It is difficult to decide how many electrodes are necessary and sufficient to identify all signal sources. For this reason, a better strategy of performing EEG analysis using ICA is to set the number of output channel to be equal to the number of input channels and then focus on the components that have large projections on the scalp and ignore those with small magnitude in projection. This is based on a simulation study performed by Makeig et al., whose results shows that when the number of sources is greater than the number of sensors, the separation of the small

component is relatively poor, while it is quite accurate in identifying the large components [23].

3.4.4 ICA Training and decomposition

To illustrate ICA training and signal decomposition we present below Figure 3.3 , which servers as a simple pictorial representation of the procedure applied to EP signal in the present research. Upper panel consists ICA training and the lower panel illustrates the signal decomposition

In Figure 3.4 upper panel, the observed signal **x**, which is the EP epoch recorded from the scalp in response to the stimuli, is fed into to the ICA algorithm. It is used to train the unmixing matrix **W**, by maximizing the entropy of the nonlinearly transformed output, **g(Wx)**.

During the decomposition (Figure 3.4 , lower panel), the EP signal recorded by **N** electrodes is decomposed into **N** independent components. The data is reconstructed with the **W** estimated during training. The row vectors of **W** can be viewed as a fixed linear spatial filter: When we pass the EP signal **x** through these filters, we have the output **u** according to equation (3.1.2 .1). Output **u** is also termed as "activations" of various components, because it represents the time course of each component.

Activations= Wx (3.4.4.1)

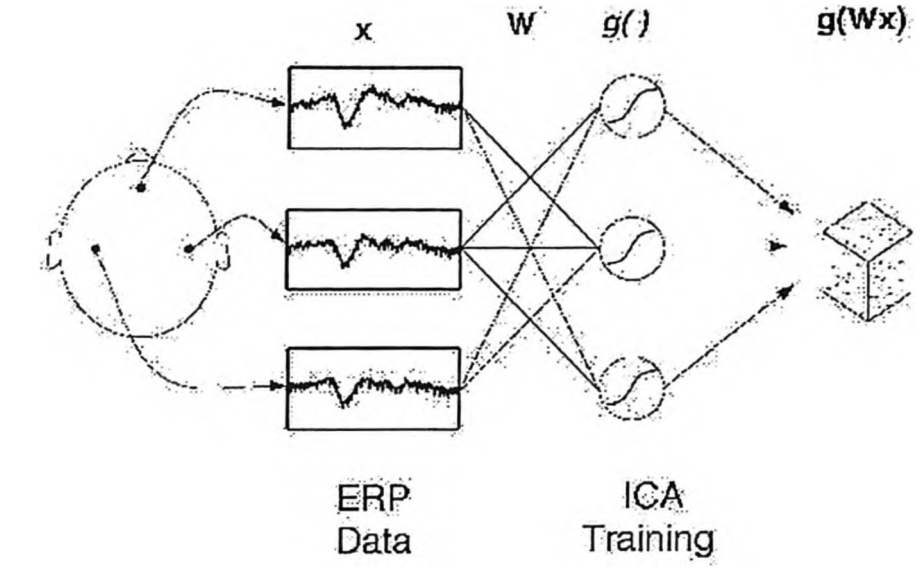

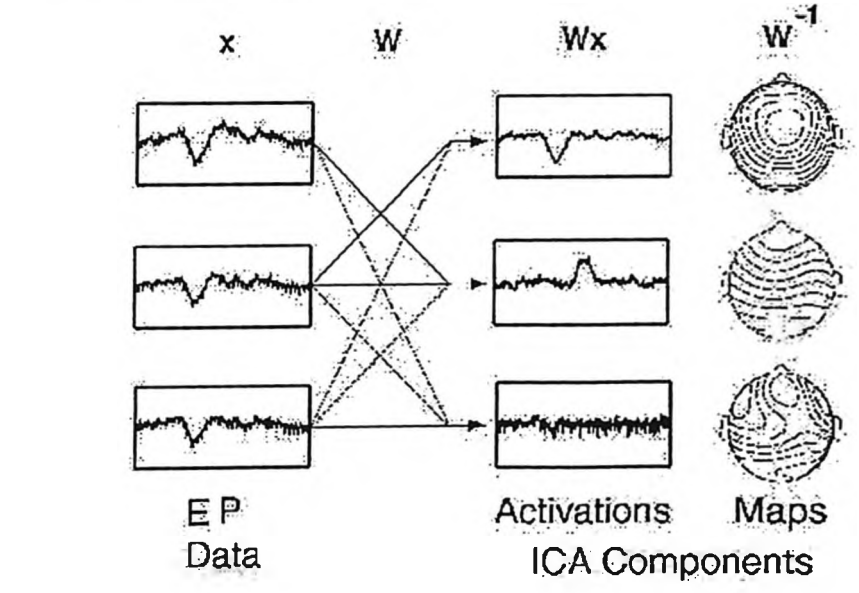

Figure 3.4 Model of implementing ICA in to EEG or EP analysis [18]

We can choose different combination of component activations to reconstruct the input signal. Such reconstruction is also known as projection of the components. This is because the reconstruction (projection) represents contribution of ICA components to the original scalp signal. It is produced by first zeroing out all but the chosen component in the activation matrix, then multiplying by the inverse weight matrix

Projection= W^{-1} Activations (3.4.4.2)

In equation(3.4.4.2), the W^{-1} represents the strength of the components in the reconstructed data. For this reason W^{-1} is plotted as a topographic map to show the fixed pattern of strengths at each scalp electrode. Although this map is not a location map for the EP component (since it doesn't show the location of the component) we can use it to characterize various components of the EP signal.

When we study the output components, we mainly study their activation and topographic map.

3.5 Conclusions

ICA is a very efficient and innovative tool for EEG and evoked potential analysis. It has the potential of solving several interesting problems associated with identifying the number of sources, source separation and therefore, provides different information that was not available before.

Chapter 4

Acquisition of human Evoked Potential Signals and Implementation of Independent Component Analysis

In this research, we demonstrated how ICA is applied to experimentally recorded human evoked potential signals. We present the details of laboratory set up, experimental protocol and how the EP signals are recorded under controlled conditions in this chapter. We will also explain how the ICA algorithm is implemented.

4.1 Evoked Potential signal acquisition

4.1.1 Apparatus for Electrical Stimulation

4.1.1.1 Stimulation electrodes

The stimulating electrode consists of 0.2mm (diameter) stainless-steel wire attached to the tip of a polyvinyl catheter and fixed with surgical silk. The catheter is 85 cm long and 5 mm in diameter. The catheter is inserted into the esophagus through a nostril. The stimulating electrode is placed about 33 cm from nostril [30, 42]. The

electrodes are connected to a Programmable Stimulation Unit (CSH Design Inc, New Maryland, NB, Canada) with a shielded electrode cable. A reference electrode is placed on the epigastric abdominal wall, about 5 cm below the xiphoid process, over the linea alba [33]. The stimulus electrode is set negative in order to stimulate the biomedical sensors receptors on the wall of esophagus. The quality of electrode contact was verified by measuring the impedance across the electrode, before and after each study. This impedance was between 0.5 kΩ to 3.6 kΩ for all subjects.

4.1.1.2 Stimulus parameters

Optimal electrical simulation parameters are chosen according to previous studies in our laboratory [43,44,45]. These parameters include duration, intensity, and frequency of the stimulus waveform. In the present research, the stimulus duration is set to 200 μs. If the stimulus duration is too long, it may cause muscle contractions. On the other hand, if the duration is less than 150 μs, adequate number of fibers may not be stimulated to generate a cortical potential. Another important parameter to be considered is the stimulus intensity. It is known that the amplitude of esophageal evoked potential is intensity dependent [41]. When stimulus intensity is smaller than the threshold, which is about 7 mA for normal subjects, the magnitude of the response to the stimulation is too small to be recorded. This is likely due to the fact that adequate number of sensory fiber are not stimulated at or below 7 mA. On the other hand, if the intensity is higher than a certain value (~ 25 mA) , it will likely cause pain. The objective of this research is to study evoked potentials below pain thresholds. In our experience no subject experienced pain during any of the stimulation protocols. Experimental results show that the

amplitude of the response increases linearly between the threshold (~7 mA) and 16 mA and tend to remain flat until 25 mA for healthy controls [41]. Based on these observations we choose 15.2 mA as stimulus intensity for the present series of experiments.

The stimulus frequency can also have a significant effect on the amplitude and latencies of peaks various and morphology of the esophageal evoked potential. There is a progressive decrease of EP amplitudes , as the stimulus frequency increases from 0.1 Hz to 1.0 Hz. Moreover, mean latencies of the principal peaks (P2, P3) shorten when the stimulus frequency increases. The phenomenon of decreasing EP amplitude with the stimulating frequency may reflect an alteration of processing of stimulus related signals between thalamic structures and cortical association fields (Ref 42). The research done in our laboratory suggests that electrical stimulation in the range of 0.1-0.2 Hz may provide optimal esophageal EP stimulus pulses. Therefore we choose 0.2 Hz in for the present study.

Besides the periodic stimulation, we also use random stimulation for this research. The random stimulation is set such that its mean frequency was 0.2 Hz with a 10-percentage variation . It is believed that random stimulation makes the subjects more alert when compared to the periodic stimulation, and the noise due to alpha (α) rhythm within the EEG signals can be depress and the speed of adaptation of EP waveform can be slowed down.

Each recording contains twenty-four stimuli, for both periodic and random protocols. This number is chosen based on experience in our laboratory. If there are too many stimuli, the adaptation will diminish the evoked response. If there are too few

stimuli, there will not be enough number of single stimulus EP signals epochs for averaging [53].

4.1.2 EP Signal Acquisition

The recording is performed in a quiet environment with lights dimmed to reduce extraneous inputs. The subject is in supine position and is required to remain awake throughout the study. During recording the subject is asked to fix his eyes on a stable target, to minimize potentials generated due to a movement of eyeballs. The subject is also instructed to avoid swallowing, because the electrical potentials generated thereby may overwhelm the EP signals. Each stimulus session lasts approximately 150 seconds. And between stimulating sessions the subject is given a break of five minutes.

The EEG signal containing the EP waveform is picked up by twenty electrodes placed on scalp according to the International 10-20 system. This corresponds to the required number of input channels (**N=20**) in the discussion of chapter 3. Two reference electrodes are placed on both combined mastoids, and a ground electrode in on the forehead. The impedances of the recording electrodes are less than 5 kΩ. The EEG signals are passed through SynAmps amplifier and handled by software named NeuroScan (Neurosoft Inc, Sterling, Virginia, USA). The gain of the amplifier is set to 500, and the accuracy is 0.168μV. The band pass filter is set between 0.15 Hz to 100 Hz.. The recording epoch is from −100 msec to 500 msec [33,49,50]. The sampling rate of the A/D converter is 1000 samples per second.

4.1.3 Data Sets

There are 41 sets of EP signals obtained from healthy controls (**n** = 4) and patients (**n** = 4) in this research. Control subjects were not is under any medication at the time of study. Table 4.1 presents the list of data sets obtained from each subject:

Study No	Recorded Date	Data Set Name	Control/Patient	age	Sex	Number of recording	Number of recording
						periodic	Random
1	28-Sep-2000	Gt0928	Control	41	M	2	2
2	5-Oct-2000	Rl1005	Control	23	M	3	2
3	31-Oct-2000	Db1031	Patient	49	F	3	2
4	17-Nov-2000	Yy1117	Control	19	M	3	2
5	17-Jan-2001	Ve0117	Control	30	M	3	3
6	24-Jan-2001	Tk0124	Patient	27	M	3	2
7	19-Mar-2001	PL0319	Patient	43	M	3	3
8	4-May-2001	HL0405	Patient	41	M	3	2
Total	41					23	18

Table 4.1 List of EP signal datasets

One of the periodic EP signals from subject No1 are plotted together with its scalp distributions in Figure 4.1. The ICA analysis is implemented in all data sets to test the algorithm

4. 2 Extended Infomax ICA implementation

In this research, the extended infomax ICA is performed. The basic ICA implementation was made available to us from Dr Makeig's lab and was modified to suit our application. The block diagram of the algorithm is shown in Figure 4.2.

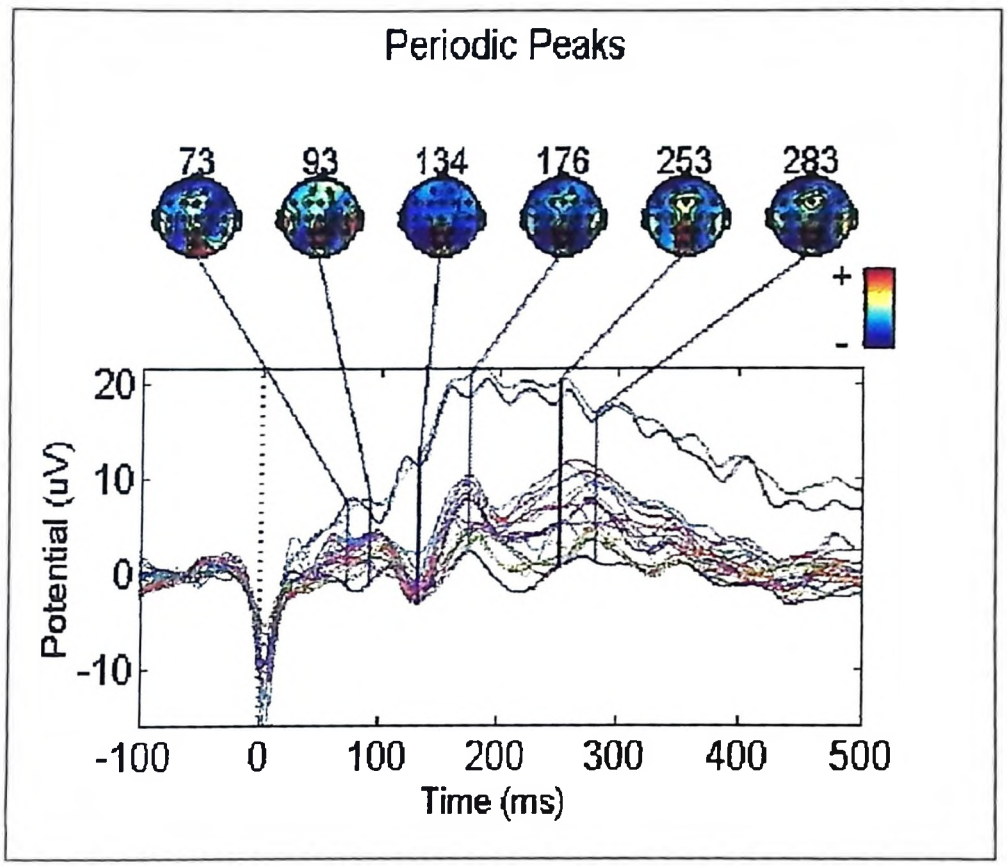

Figure 4.1 Twenty channels of esophageal evoked potential signals and scalp distribution of main peaks: N1 (73 ms), P1 (93 ms), N2 (134 ms), P2 (176ms), N3(153 ms), P3(283 ms)

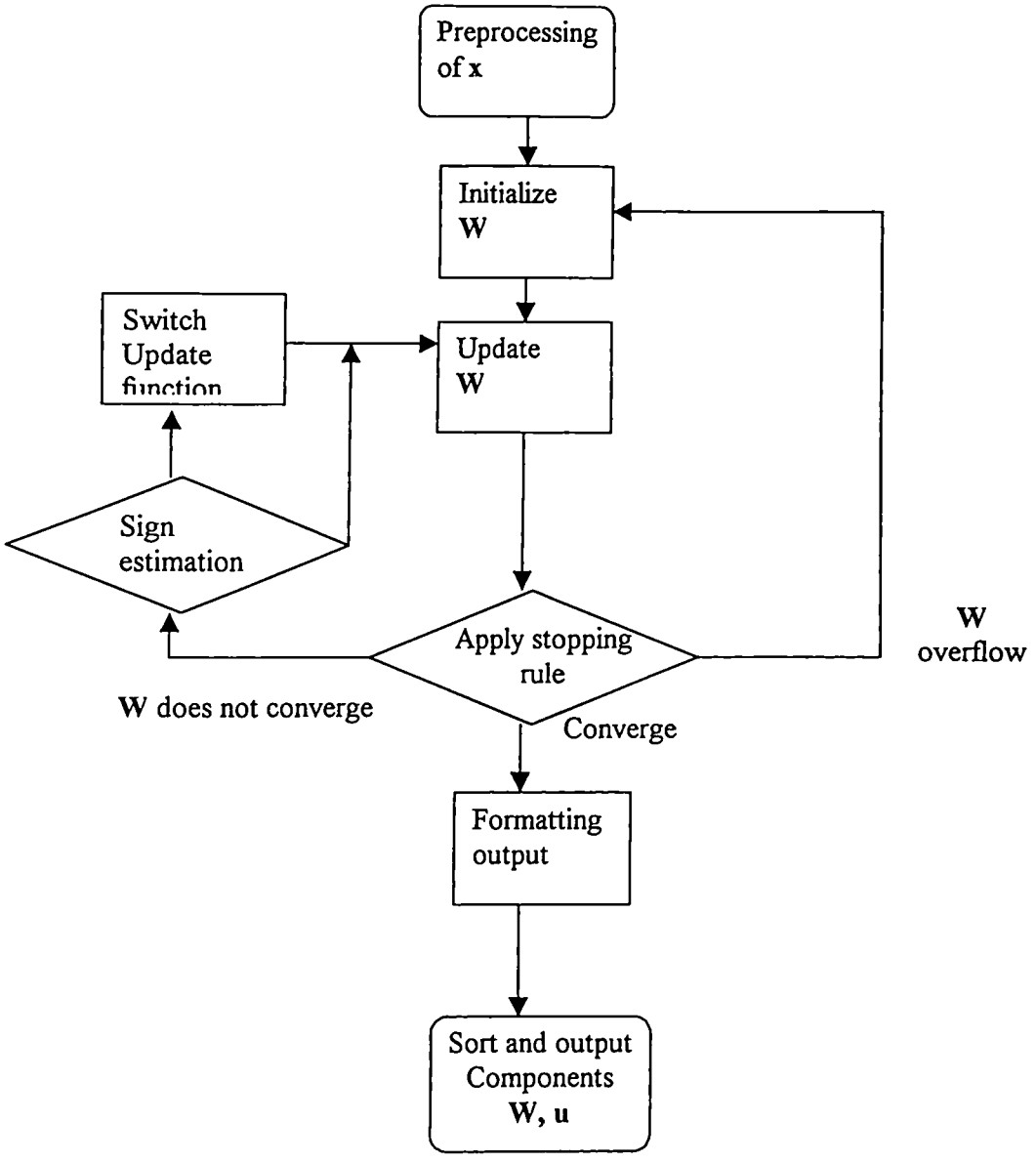

Figure 4.2 Block diagram of the extended infomax ICA algorithm

4.2.1 Preprocessing

The Evoked Potential signals are reformatted into a 20x600 matrix, corresponding to 600 ms data from 20 channels. This corresponds to the observed data **x** in the discussion of chapter 3, which is input data to the ICA algorithm. The first and second-order statistics of the data should be removed before training in order to make the convergence more stable. Otherwise the training noise will swamp the higher order statistics [1]. To remove the fist order statistics: mean of the signal is given by equation (4.2.1.1) is subtracted.

$$\mathbf{m(x) = E\{x\}} \tag{4.2.1.1}$$

This also makes the output components have zero-mean. If needed, we can correct this in the formatting output block in figure 4.2, by adding the mean vector of **u** to the centered estimates of output **u**. The mean vector of **u** is given by

$$\mathbf{m(u) = W\ m(x)} \tag{4.2.1.2}$$

The sphering is done by multiplying the decorrelating matrix with the zero-mean input data

$$\mathbf{x = Sx} \tag{4.2.1.3}$$

where the decorrelating matrix S is given by

$$S = 2\langle xx^T \rangle^{-1/2} \tag{4.2.1.4}$$

This decorrelation is called zero-phase decorrelation or whitening, which constrains the matrix to be symmetric. Compared with other popular whitening techniques such as Principal Component Analysis (PCA), which constrains the matrix to be orthogonal, the

zero-phase decorrelator is non-orthogonal, and gives much better starting points than the PCA [50]. Theoretically, the sphering is not necessary for the natural gradient, but it is implement because the convergence is more stable on sphered data.

4.2.2 Initializing and updating

Before ICA training, **W** is initialized to the identity matrix **I**, as recommended by Bell at al [36].

According to extended infomax ICA, the update equation for **W** is different for super-gaussian and sub-gaussian signal source. As derived from equations (3.3.4.4) and (3.3.4.5), the update rule for **W** is

$$\Delta W = \varepsilon (I - K \tanh(u). u^T - u u^T) W \qquad (4.2.2.3)$$

For **K**, $\begin{cases} k_i = +1 & \text{for super-Gaussian source} \\ k_i = -1 & \text{for sub-Gaussian source} \end{cases}$

This switching is performed in the sign estimation block in figure 4.2, where the k_i is estimated with equation (3.3.4.5), and is given by:

$$k_i = \text{sign}(E\{\text{sech}^2(u_i)\} E\{(u_i^2)\} - E\{\tanh(u_i). u_i\})$$

The learning rate ε is normally set to <0.01, in our experiment. It is chosen empirically:

$$\varepsilon = 0.015/\log(\text{Number of channel}) \qquad (4.2.2.4)$$

The ε is equal to 0.0115 in our study, for N=20 signal channels.

The computed update is based on small batches of randomly selected data vectors drawn from input data set **x**. The batch size is chosen according to the equation:

$$\text{batch size} = \text{floor}(\text{sqrt}(\text{timepoint}/3)) \qquad (4.2.2.5)$$

This is suggested by Bell and Sejnowski [51]. Based on equation (4.2.2.5), since our signal has 600 samples for each channel, the batch size is set to 14.

After each pass through data points, an angle representing the difference in direction between the update vectors in the current and previous passes is computed. Whenever this angle is larger than 60 degree, the learning rate is reduced by 2 % [22].

4.2.3 Stopping rule and formatting output

The training stops when the learning rate decreases below 0.000001, which implies the change of **W** has stabilized. Or if **W** blows up, which happens when the elements of **W** become very large, i.e. 10^8, the training will restart with a lower learning rate.

The components are sorted by descending order of mean projected variance. The projection is computed by (3.4.4.2) then for each output component **i**

$$\textbf{Projection (i)= (SW)}^{-1}\textbf{ (i)*Activations(i)} \qquad (4.2.3.1)$$

Since the original data is multiplied by the decorrelating matrix **S** before, the $\mathbf{S^{-1}}$ is used when we compute the projection. And the mean variance is

$$\textbf{Mean Variance = mean (}\Sigma\textbf{(Projection(i).* Projection(i))/n)} \qquad (4.2.3.2)$$

Where **n** is the number of time point in each channel.

4.2.4 Summary

In this chapter we have outlined recording procedure to obtain reproducible esophageal evoked potentials. An outline of the ICA computation is also presented.

Chapter 5

Results

In this chapter, we will describe the results of subjecting esophageal evoked potential signal to independent component analysis. We intend to study the reproducibility, artifact removal and examine the common components present in the averaged evoked potentials generated due to both periodic and random stimulation applied to the human esophagus.

5. 1 Evoked Potential Signal Processing

In this research, all signal analysis is performed using Matlab 5.01 software on a Dell Dimension XPS B866 PC with 866 MHz processor. Initially the extended ICA decomposition is applied to each averaged EP signals as well as to the grand averaged signal obtained from each subject. The initial learning rate started at ~0.0115 and gradually reduced to 10^{-6} during 100-300 training iterations that required ~15 seconds of computer time. The component map and activation matching are performed by computing their correlation coefficients (CC). The correlation coefficient is a measure of

how closely two variables or waveforms are correlated. For example, denote vector **x** and **y** as vectors that are used to generate component maps, then their correlation coefficients can be computed by :

$$r = \frac{\sum (x_i - m_x)(y_i - m_y)}{\sqrt{\sum (x_i - m_x)^2 (y_i - m_y)^2}} \qquad (5.1.1)$$

where i=1,2...n , (n is the number variables in the vector); $\mathbf{m_x}$ is the mean of **x** and $\mathbf{m_y}$ is the mean of **y**

The values of the coefficient can range from -1 to +1. When the components maps look similar, their correlation coefficients are high (>80%). A second measure of variation of the EP signals naturally, the coefficients of variation (CV) of the CC is computed, which is given by the equation

CV=((standard deviation)/mean of CC)*100% (5.1.2)

The rationale for using correlation coefficients and CV to study reproducibility, is that if **r** is large and close to 1.0 across different data sets, then the components under consideration is reproducible. Alternatively, if CV is small (<20%), then there is minimal variation across different trials conducted for studying reproducibility.

5. 2 Within Subject Reproducibility

In this section, we intend to test if the result of the extended ICA decomposition is reproducible. Initially, for each periodic stimulation session (n=24 stimuli) an averaged EP signal was computed. This was repeated three times (denoted by P1, P2 and P3) as described in section 4.1 of Chapter 4. A grand average of the EP signal generated from these three stimulus sequences was also computed for comparison. Extended ICA

algorithm was used to compute independent component set for each stimulus sequences (i.e. P1, P2 and P3). Each component set contains 20 component maps and their activation waveforms. A fourth component set was generated out of the EP signal arising out of the grand average of these three stimulus sequences (averaged response to P1, P2 and P3 stimulus sequences). Next, the highest-correlated pair of the component maps, i.e. those with the highest correlation coefficients, are determined and tabulated for each subject. We repeated the above procedure until all 20 successively decreasing correlated pairs are found. Subsequently, the average correlation coefficient for each component is computed and its coefficient of variation (CV) is determined. The same procedure was repeated for random stimulation sequences. Thus all 41 datasets (23 periodic and 18 random) were analysis as described above. Table 5.2.1 is a typical representation of correlation coefficient and CV of EP signal recorded from subject No.7, to random stimulation. The table is sorted by the mean correlation coefficient of the components, which lists the highest matching component at the top. The scalp distribution maps of four of the twenty components are highlighted in Table 5.2.1 and shown in Figure 5.2.1 . These maps demonstrate the effect of matching using correlation coefficients and CV. The components in the upper two rows are highly reproducible. The mean correlation coefficient in each row is greater than 0.80 and CV are less then 20%. The components in lower two rows are components which have poor reproducibility ($r<80\%$ and $CV>20\%$).

AVG	Random 1			Random 2			Random 3			Mean
Comp.No.	Comp.No.	r	CV	Comp.No.	r	CV	Comp.No.	r	CV	r
1	1	0.986	0.0066	1	0.9932	0.0007	1	0.9983	0.0058	0.9925
2	7	0.9471	0.0144	2	0.9514	0.0099	2	0.9842	0.0243	0.9609
4	9	0.9069	0.0244	4	0.9063	0.0251	6	0.9757	0.0495	0.9296
11	13	0.9348	0.0234	3	0.8502	0.0692	5	0.9553	0.0458	0.9134
5	15	0.9403	0.0342	6	0.876	0.0365	8	0.9114	0.0024	0.9092
3	2	0.9259	0.0335	7	0.8069	0.0993	12	0.9547	0.0657	0.8958
7	12	0.9508	0.0987	8	0.855	0.0121	7	0.7906	0.0865	0.8654
17	3	0.952	0.1224	11	0.788	0.071	13	0.8045	0.0514	0.8482
6	8	0.9668	0.161	10	0.6201	0.2554	4	0.9115	0.0944	0.8328
13	4	0.8858	0.1032	9	0.9034	0.1252	10	0.6196	0.2284	0.8029
8	5	0.8631	0.0851	5	0.831	0.0447	18	0.6921	0.1299	0.7954
9	14	0.846	0.124	12	0.7852	0.0432	15	0.6269	0.1672	0.7527
12	18	0.8676	0.1686	13	0.5133	0.3087	3	0.8465	0.1401	0.7424
16	17	0.8615	0.3149	14	0.8547	0.3045	20	0.2494	0.6194	0.6552
18	16	0.7368	0.6345	16	0.0823	0.8618	19	0.5532	0.2273	0.4508
14	10	0.707	0.7621	20	-0.3869	1.9643	11	0.8836	1.2022	0.4012
10	11	0.9033	1.3427	19	-0.2916	1.7562	14	0.545	0.4134	0.3856
20	6	0.3748	0.0339	18	0.5386	0.4859	9	0.1741	0.5197	0.3625
19	20	-0.1219	1.4129	17	0.1202	0.5928	17	0.8871	2.0057	0.2951
15	19	-0.4709	3.9536	15	0.4054	1.5427	16	0.5438	2.4109	0.1594

Table 5.2.1 Matching result of component map from esophageal EP of random stimulation of subject No.7.

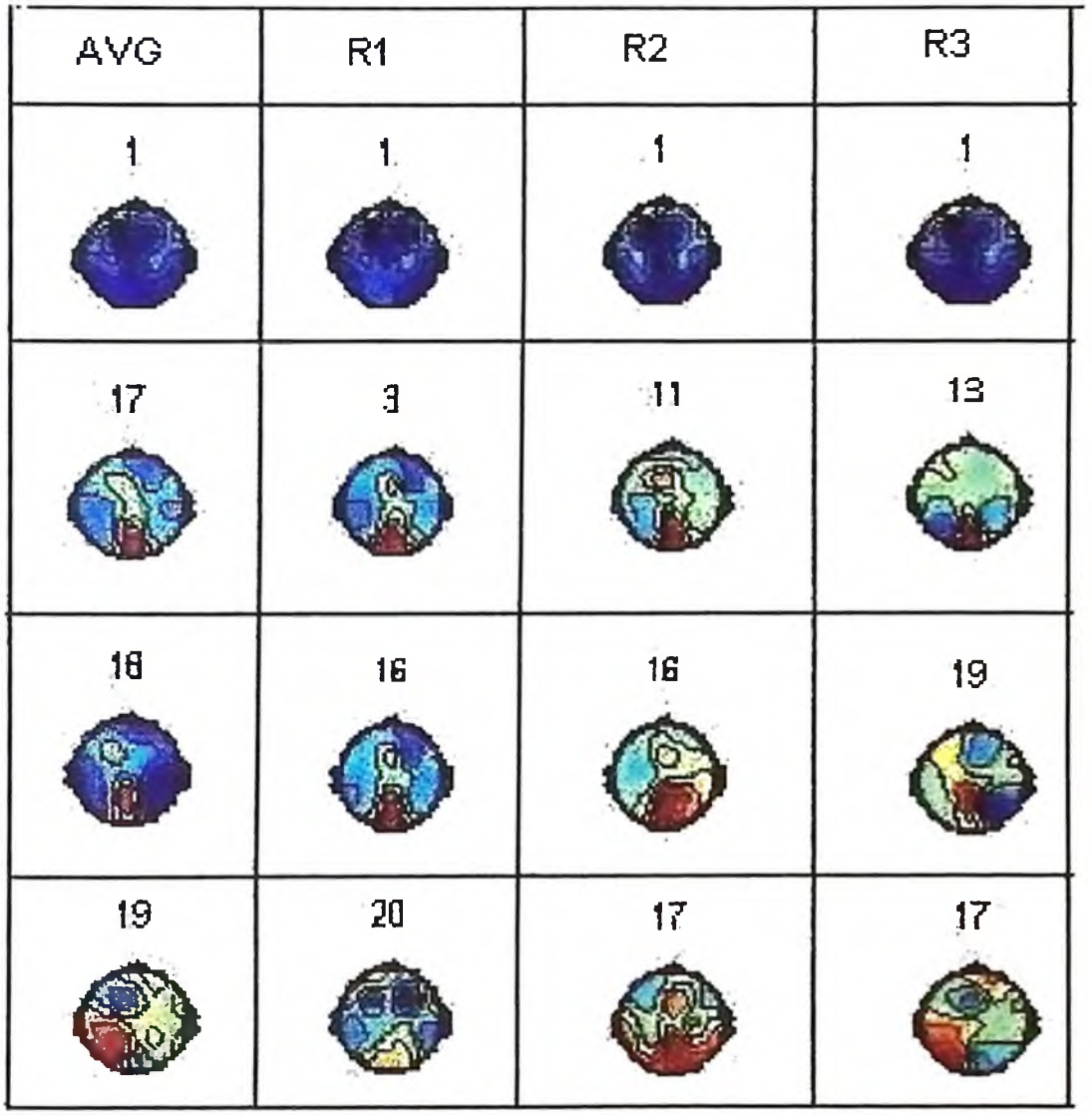

Figure 5.2.1 A typical set of matching samples of component map from esophageal EP of random stimulation of subject No.7.(R1, R2, R3 are random stimulus sequences) Top two sets of component have high reproducibility ($r>0.8$,$CV<20\%$) Lower two sets of components have low reproducibility ($r<0.8$, $CV>20\%$). (Refer to table 5.2.1.)

For the periodic stimuli, we note that between 6-14 components are found to be highly reproducible (r>80% and CV<20%) within each subject. For the random stimulus paradigm, number of reproducible components varies between 6 to 12, for different subjects. These results are summarized in the following table:

Subject No	Data Set Name	Number of Reproducible Components	
		periodic	Random
1	Gt0928	14	7
2	RI1005	9	11
3	Db1031	7	10
4	Yy1117	7	6
5	Ve0117	9	8
6	Tk0124	7	12
7	PL0319	6	10
8	HL0405	12	8
Mean		~9	9

Table 5.2.2 Number of reproducible components within each subject

These observations suggest that approximately 9 out of 20 components are reproducible for both periodic and random stimulation protocols.

5.3 Removal of the Stimulus Artifact From the Averaged Evoked Potential Signal Using ICA

A consistent and reproducible artifact is generated on the cortex by the electrical stimulus. This artifact shows up within the first 15 ms following the stimulus in all channels of the EP signal and in all subjects. This phenomenon can be demonstrated

through Figure 5.3.1, the normalized power ratio of the stimuli artifact in a typical subject (Subject No.1). The normalized power ratio is computed as the power within a channel but normalized to highest amplitude of the signal across all electrodes. In this subject, the artifact power is distributed in all EP signal channels but predominantly in frontal channels (F7, F8, Fp1 and Fp2). Such artifact was concentrated in one component following the extended ICA decomposition. This artifact component can be identified by examining the activation of the component waveforms. Furthermore, computing the power ratio of all the component projections between 0-15 ms can confirm this observation. Results for subject No. 1 is shown in Figure 5.3.2, the first component has the dominate power compared to all the other components, which implies that it is the stimulus artifact.

Since channel Cz is one of the most commonly used channels to study esophageal EP signals, we demonstrate the effect of removing the stimulus artifact component on the EP signal for that electrode. Figure 5.3.3 is the projection of stimulus artifact component in channel Cz. The waveform shows that this component contributes to the activation between 0 to 15 ms. Figure 5.3.4 is a comparison between the original signal and the signal reconstructed with all the other component but without the stimulus artifact.

The removal of stimulus artifact component is a clear evidence that ICA algorithm provides functional separation of different components within the esophageal EP signal. Since we know that the stimulus artifact is from sources independent of the EP signal generators, Figure 5.4.4 demonstrated that such artifact can be extracted fully using extended ICA decomposition. We believe this experimental evaluation of the algorithm verifies its validity and separability of independent components..

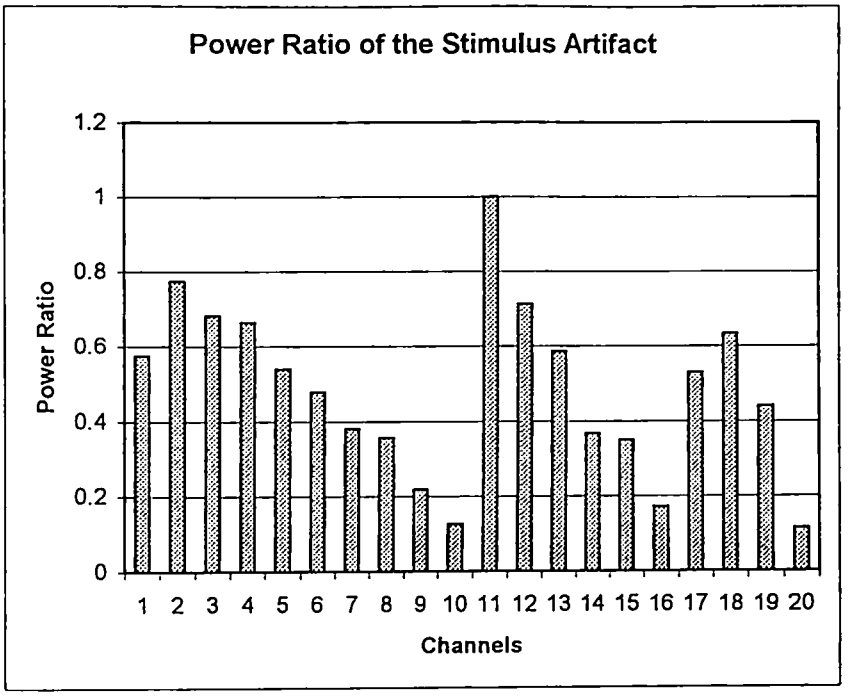

Channel No.	Channe Name
1	FP1
2	FP2
3	F3
4	F4
5	C3
6	C4
7	P3
8	P4
9	O1
10	O2
11	F7
12	F8
13	T3
14	T4
15	T5
16	T6
17	CZ
18	FZ
19	PZ
20	Oz

Figure 5.3.1 Normalized Power Ratio of the stimulus artifact in original esophageal EP signal from subject no.1

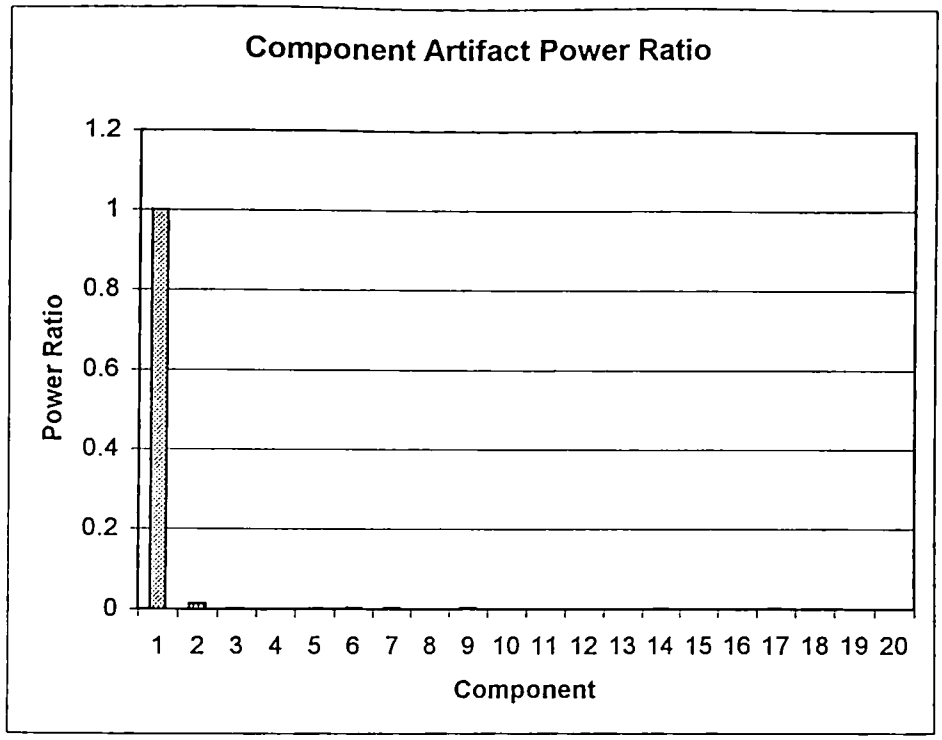

Figure 5.3.2 Normalized Power Ratio of the stimulus artifact in ICA components from esophageal EP signal for subject no.1

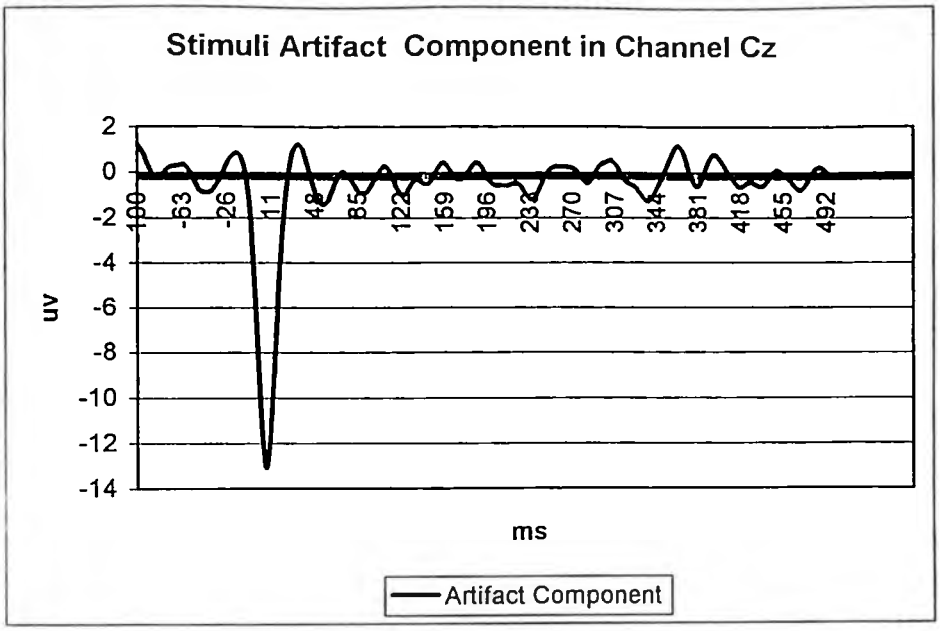

Figure 5.3.3 Stimulus Artifact component projection in channel Cz.

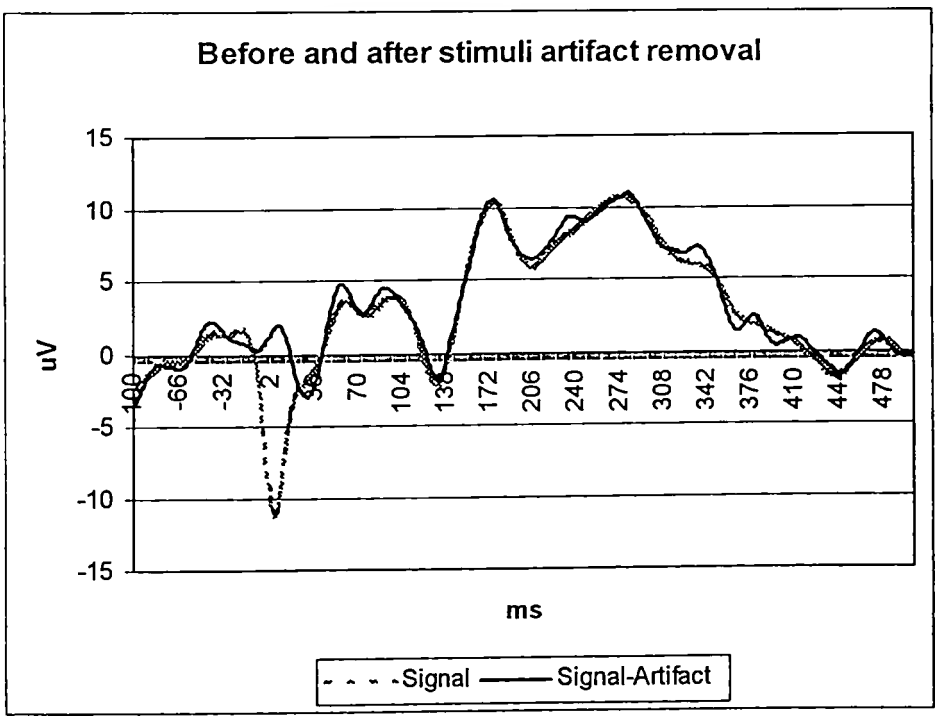

Figure 5.3.4 Comparison between original signal and signal reconstructed without stimuli artifact component in channel Cz.

Besides the component attributed to the stimulus artifact there are three other components that present strong activation before the stimulus (0 ms) in their activation waveforms. These are due to noise and were removed from further study.

5.4 Comparison between the ICA components of the EP signal due to periodic stimulation and random stimulation

5.4.1 Comparison of ICA components across subjects but within the same stimulation protocol

In order to compare different components arising out of the ICA algorithm in response to identical stimulation protocols, we examined correlation coefficients of different activation waveforms as well as their maps across all subjects. Components with highest correlation coefficients were identified and listed in Table 5.4.1.1. It was noted that certain components appear at distinct latencies in four or more subjects with high correlation ($r>0.9$). These components were verified visually by examining the activation waveforms. A sample set of the waveforms from two subjects is show in Figure 5.4.1.1.

Periodic Component	Mean of max peak latency (ms)	Number of Subject	Mean CC. of Activation
CP1	59.50	4	0.9563
CP2	93.57	7	0.9361
CP3	129.38	7	0.9500
CP4	150.60	5	0.9568
CP5	174.20	5	0.9186
CP6	282.00	4	0.9458

Table 5.4.1.1 Reproducible components across subjects in EP signal of periodic stimulation

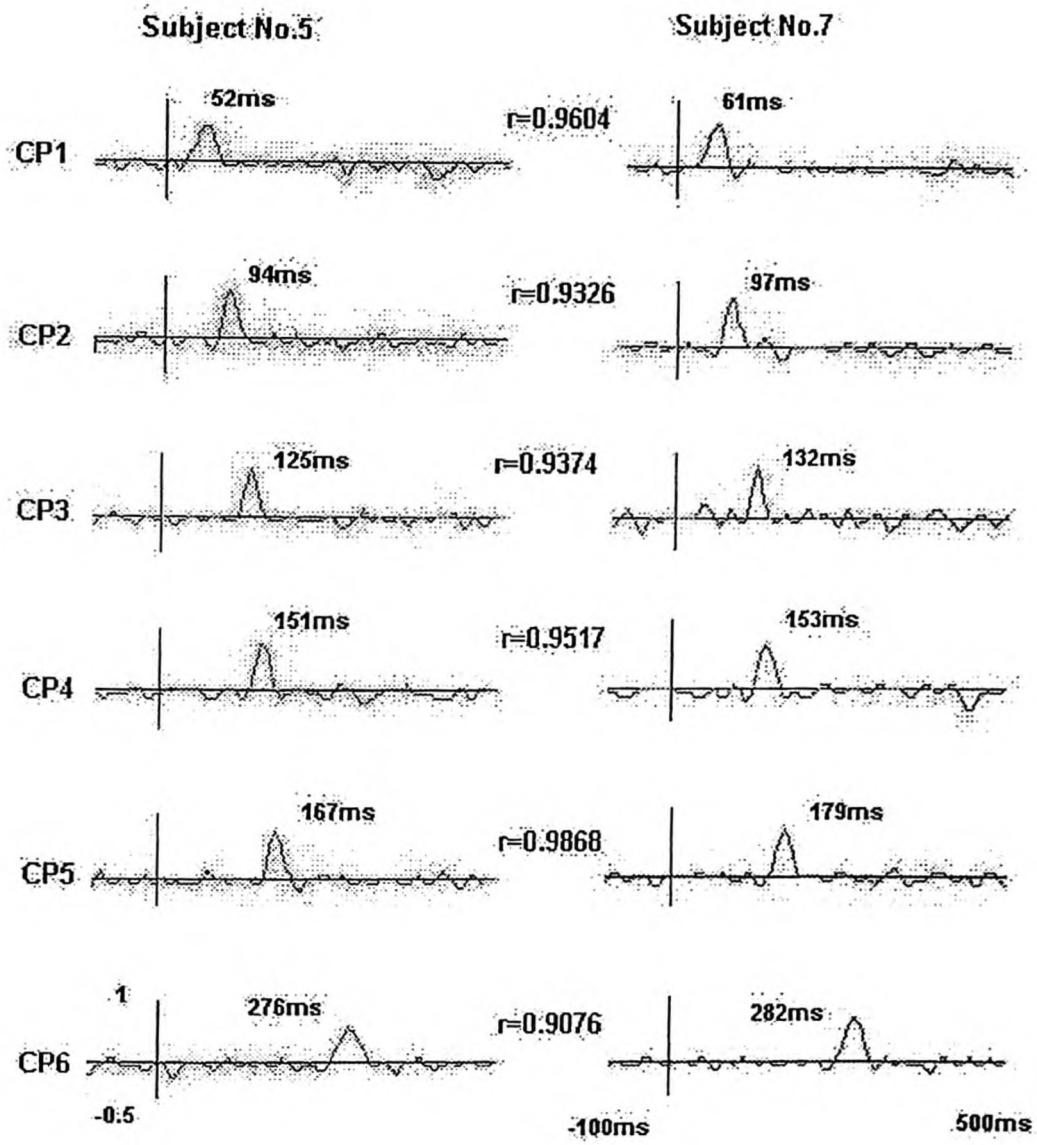

Figure 5.4.1.1. Activation waveforms of reproducible components due to periodic stimulation from subject No.5 and subject No 7.

Random Component	Mean of max peak latency (ms)	Number of Subject	Mean CC. of Activation
CR1	84.71	7	0.9630
CR2	127.20	5	0.9896
CR3	143.00	7	0.9423
CR4	208.11	8	0.9021
CR5	240.86	6	0.9424
CR6	265.40	4	0.9437
CR7	256.71	5	0.9824
CR8	374.14	7	0.9032

Table 5.4.1.2 Reproducible components within the EP signal of random stimulation and across subjects

A similar analysis performed on random stimulation protocol yielded a slightly different result (table 5.4.1.2) indicating that certain components are highly reproducible across different subjects for random stimulation. However, latencies of their activation are different from those due to periodic stimulation, an issue examined in greater detail below.

5.4.2 Comparison of activations and maps across subjects for different stimulation protocols

Since the components due to periodic and random stimulation protocol seemed to appear around the same latency, we computed correlation coefficients of activation waveforms for the component listed in table 5.4.1.1 and table 5.4.1.2. It is interesting to note that the component responding to random stimulation seem to appear a few

milliseconds before a related component due to periodic stimulation, perhaps suggesting that response to random stimulation is generated more rapidly within the nervous system

Periodic		Random		Mean CC of Activation
Component	Mean of max peak latency	Component	Mean of max peak latency	
CP2	93.57	CR1	84.71	0.9320
CP3	129.38	CR2	127.20	0.9442
CP4	150.60	CR3	143.00	0.9393
CP6	282.00	CR6	265.40	0.9617

Table 5.4.2.1 Common components of esophageal EP signal from periodic and random stimulation (CP stand for components obtained from the periodic EP signal, and CR for those of random EP signal)

The activation waveforms and scalp distribution map of these component pairs are plotted in Figures 5.4.2.1-5.4.2.4

5.4.3 Study of Common Components for periodic and random stimulation

5.4.3.1 CP2 and CR1

Figure 5.4.2.1 plots the activation waveforms of CP2 and CR1 and allow easy comparison of the time courses between these two components. These waveforms are very similar in shape. Latency of the component due to the random stimulation (CR1) is 84.71 ms, whereas the latency due to the periodic stimulation (CP2) is 93.51 ms.

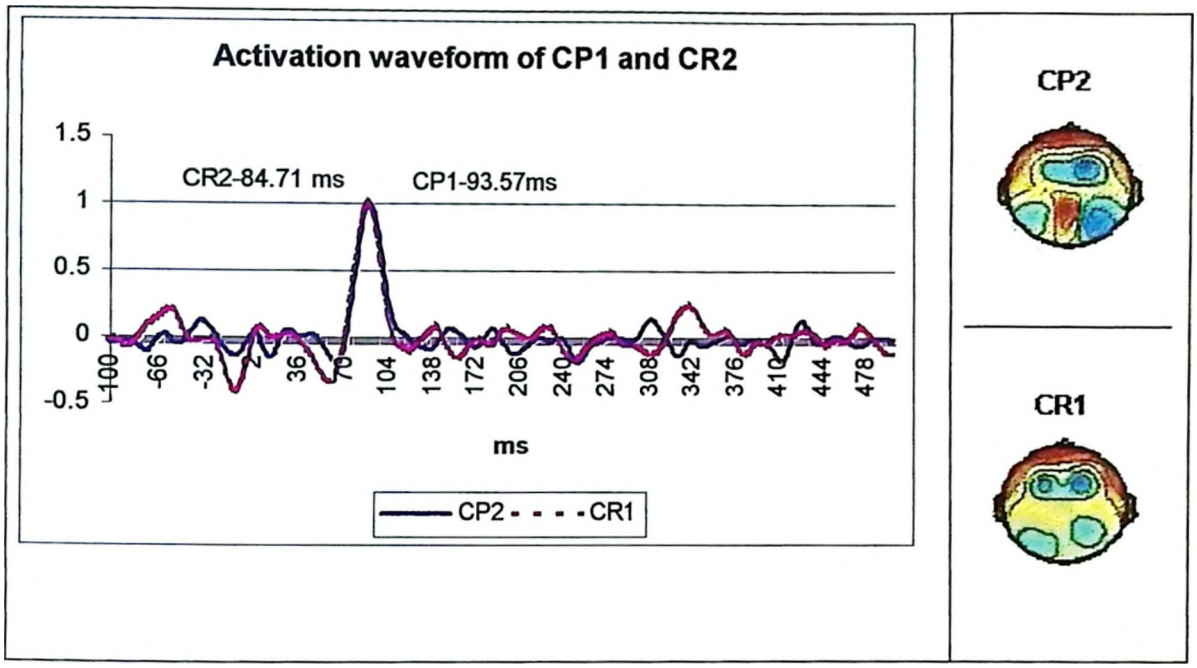

Figure 5.4.2.1Activation waveforms and maps of component CP2 and component CR1

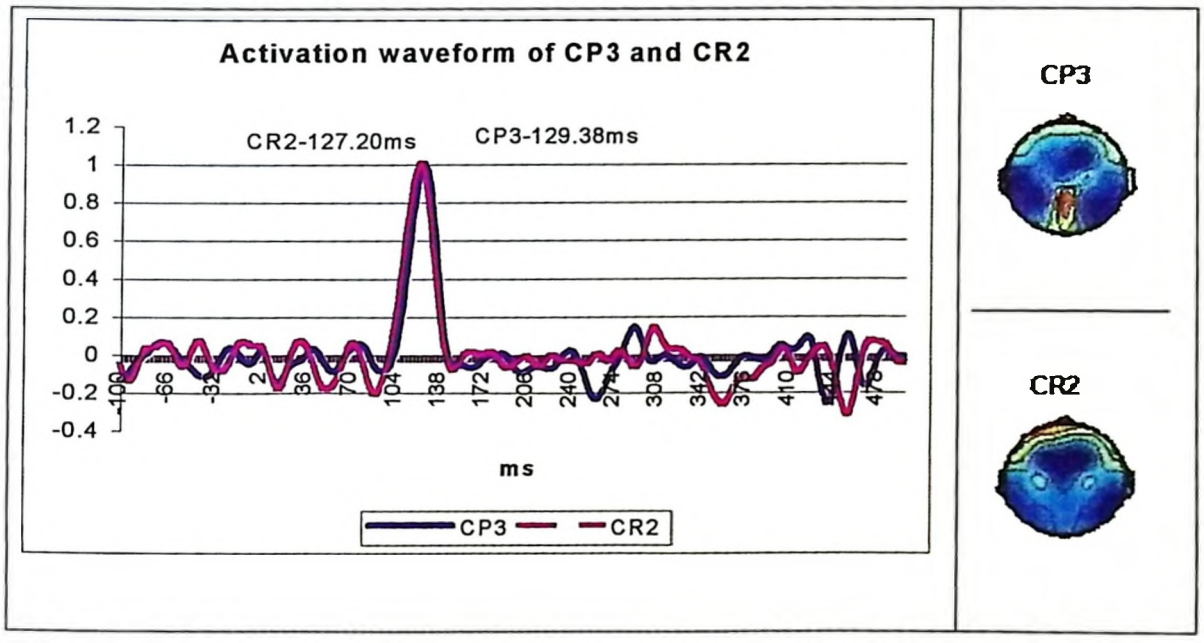

Figure 5.4.2.2 Activation waveforms and maps of component CP3 and component CR2

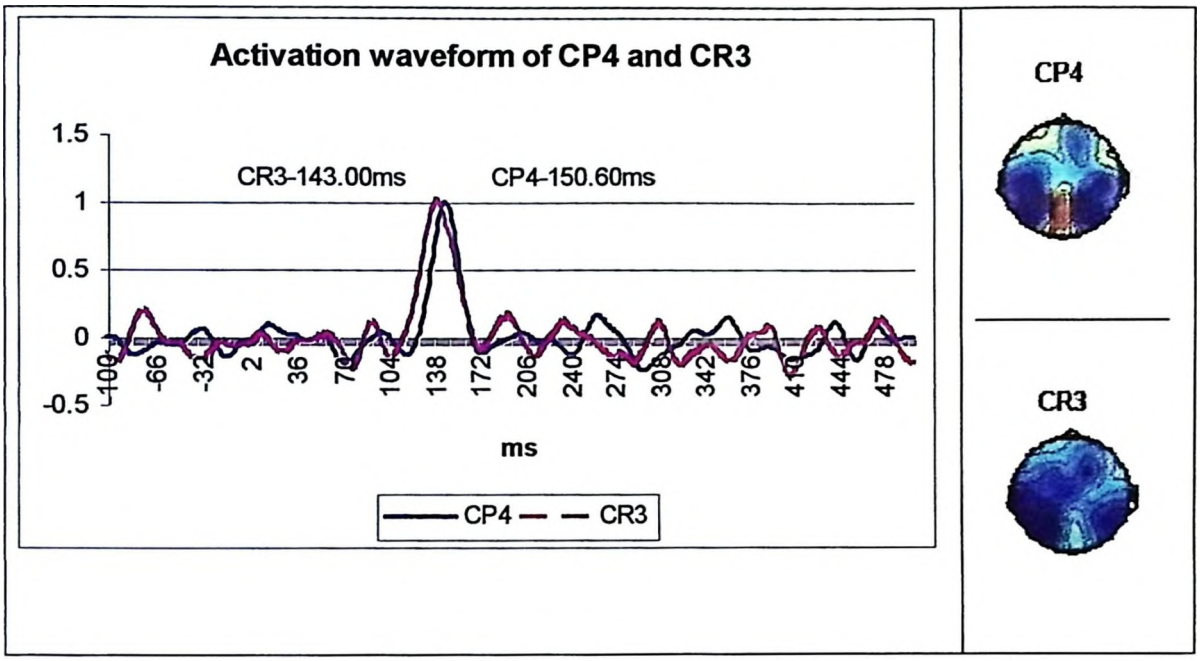

Figure 5.4.2.3Activation waveforms and maps of component CP4 and component CR3

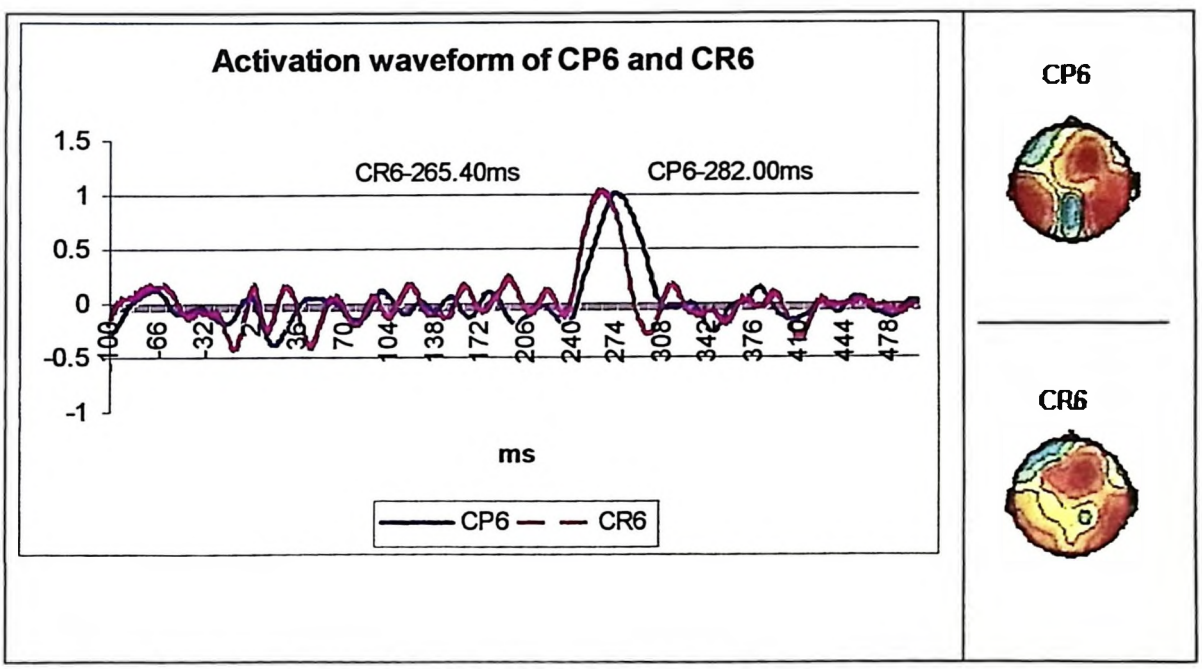

Figure 5.4.2.4Activation waveforms and maps of component CP6 and component CR6

Also, we observe that components CP2 and CR1 are perhaps related to the P1 peak in the standard averaged EP signal (Chapter 2 figure 2.3)by virtue of having a latency close to the peak at 101.9 ± 15.5 ms [30]. The scalp distribution maps of CP2 and CR1 demonstrate that these two components both have a strong positive potential in the frontal pole area and a small negative potential at T5, T6 and F4 electrode locations. However, CP2 has a strong positive activation in the mid-central and mid-parietal area while the CR1 is neutral in that area.

5.4.3.2 CP3 and CR2

The second pair of common components due to periodic and random stimulation are shown in Figure 5.4.2.2. It can be observed that their latencies are at 127.20 ms (CR2) and 129.38 ms (CP3). Their component maps show that there is negative potential all over the scalp except in frontal pole area (i.e. Fp1 and Fp2). However, the component due to random stimulation (CR2) is neutral while CP3 appears as positive in the mid-central areas. Also, CR2 seems to have a relatively higher positive activation than the CP3 in the frontal pole area.

5.4.3.3 CP4 and CR3

The component pair CP4 (150.60 ms) and CR3 (143.00ms), which are shown in Figure 5.4.2.3, appear to be activate near the N2 peak (141.1 9 ± 19.4) of the standard EP signal (Chapter 2 Figure 2.3) [30]. The activation pattern of the these two components is negative in right frontal pole and posterior temporal areas (proximity of T5 and T6

electrode). For CP4, the left frontal pole and the mid-central areas seem more active then that for CR3.

5.4.3.4 CP6 and CR6

The CP6 and CR6 component pair has almost the same activation area as CP4 and CR3, except this pair has positive potential. Furthermore, the activation of CP6 in right posterior temporal area is stronger than that of CR6. The latency of CP6 is 282.00 ms and for CR6 the latency is 265 ms. Their activation waveforms(Figure 5.4.2.4) suggests that they may related to the late response N3 at 262.3± 38 ms of the standard esophageal EP signal (Chapter 2 Figure 2.3) [30].

5.4.3.5 Summary of comparison between periodic and random stimulation

There are common characteristics in these four pair components we studied above. They are as follows:

1. The activation waveforms due to periodic stimulation show latencies later than their related components due to the random stimulation.
2. The periodic stimulation generates components with higher activation in the middle brain area (Cz and Pz electrode location) than the random stimulation.
3. Some of the selected ICA components seem related to the peaks of the standard esophageal EP signal (Chapter 2 figure 2.3), which suggests that the components due to ICA may contain functional information of interest to clinical medicine.

5.5 Summary

In this chapter, we studied the output of the extended ICA as applied to the esophageal EP signal. Analyses were performed on the reproducibility of various components. We also identified differences between components in response to random and periodic stimulation protocol. Based on our results, we believe ICA algorithm can provide functional separation of the esophageal EP signal.

Chapter 6

Discussion

In this chapter we will discuss the results reported from Chapter 5 and also present the limitations and suggestions for future research for this study.

6.1 Comparison between the ICA components of the EP signal due to periodic stimulation and random stimulation

In section 5.4.1, a comparison of latencies across subjects following periodic/random stimulation demonstrates that certain components appear at distinct time following a stimulation pulse with high correlation ($r > 0.9$). It is likely that these components may originate in the same neuronal structures and hence are reproducible across different subjects. The typical activation waveforms of the ICA components have a dominant peak within a certain time window (Figure 5.4.1.1) and do not appear any other time. This phenomenon may suggest that the response of the neuronal source is localized.

We observed that EPs studied across subjects but for different stimulation protocols (section 5.4.2) demonstrate that activation waveforms due to periodic stimulation show

latencies later than corresponding components due to the random stimulation. Such correspondence between two stimulation protocol may be due to the fact that the random stimulation protocol gives irregular stimuli that makes the subjects more alert. Thus specified peaks of the evoke response to the random stimulation is generated earlier.

The second finding of section 5.4.2 is that the periodic stimulation generates components with higher activation in the mid-brain area (Cz and Pz) when compared to components due to random stimulation. This phenomenon was not reported by any other research on esophageal EP before. It may suggest that the response of the periodic stimulation involve neurons structures slightly different from the random stimulation. However this observation needs further study with more subjects.

Figure 5.4.2.1 to Figure 5.4.2.4 also demonstrate that some of the ICA components seem related to the peaks of the standard esophageal EP signal (Chapter 2 Figure 2.3). The occurrence of peaks and similarity of the maps in EP at approximately the location (i.e. CP2 and CR1, CP3 and CR2) suggests that these peaks are generated in the same location and transmitted to the cortex along similar structures and therefore result in similar scalp distribution. The physiological meaning of these scalp maps need to be further studied.

The removal of stimulus artifact component also provides a confirmation of the analytic power of ICA, that it can decompose the EP signal into meaningful components.

6.2 Limitations and suggestions for further research

6.2.1 Choice of the algorithm

There are several criteria for estimation of the ICA model, including mutual information, likelihood, cumulants, nongaussianity measures, and nonlinear principal component analysis (PCA) criteria. Extended infomax algorithm is only one of several algorithms that can be derived from information theory. It has been shown that all these algorithms are closely connected and can be unified based on the information theoretic point of view [37, 40,46]. However, there are still differences in their performance. A. Hyvaerinen et al performed experimental comparison with stimulated data for the different algorithms including: FastICA, infomax, extended infomax and recursive least-squares algorithm for a nonlinear PCA (NPCA-RLS). Their results show that extended infomax can provide good statistical performance for separating different component, because it involves a **tanh** function in the nonlinearity, which gives the best results [55]. They also investigated as to how the statistical performance of the algorithms changes with increasing number of components. Their results show that original infomax and extended infomax achieve the best accuracies compared to the other algorithms [55]. The computational load of extended infomax ICA algorithm is relatively high. But in our study, the average converging time is around 15 seconds, which is acceptable for the present application. However, from the point of view of the robustness, the extended method has a major weakness: when many sources are close to Gaussian, the training noise will cause the learning rule to switch between the regimes of super and sub-gaussian [17]. But we did not encounter this problem in our research. Moreover, the

extended infomax algorithm has been applied to biomedical signals for many years and has proven to be useful in evoked potential signal analysis [9]. Based on the discussion above, extended infomax is practical and is a suitable ICA algorithm for the present study.

FastICA algorithm could also be deployed to examine and confirm the results of extended infomax ICA. The FastICA algorithm can deal with both supergaussian and subgaussian sources [55].

6.2.2 Addition of Electrodes

The maximum number of ICA output components depends on the number of EEG channels at the input. We are currently using twenty EEG channels as inputs in our research. Therefore, the number of output is restricted to twenty components only. Further, we could identify about nine reproducible components from each subject. There are many reasons that may result in ICA components which are not reproducible between successive trials within subjects. An important reason may be that we may have used fewer channels than the number of actual biological sources of signal. A simulation study shows that when the number of sources is greater than the number of sensors, the separation of the larger component is still quite good while it is relatively unsuccessful for the smaller components [23]. Therefore as the number of recording channels increases, we can expect more reproducible independent components from the ICA algorithm.

6.2.3 Single-Trial vs. Averaged Evoked Potential

Since we have recorded both single trial and averaged EP signals, it could be natural to consider if we can apply ICA to both instead of to the averaged EP only. There are some good reasons to do single trial EP analysis, since the response and scalp distributions successive stimulus sweeps. Those variations from stimulus to stimulus may contain useful information regarding habituation or the ability to concentrate. When we analyze the averaged data, we may be ignoring useful information. Therefore, one can argue that analysis of single-trial ERP might provide more information about brain dynamics than averaged response. However, we foresee following limitations for such analysis. First of all, single-trial EP signal has poor signal-to-noise ratio, since averaged data is able to remove those non- time locked artifacts, but single trial signal contain all of them. If we apply it into ICA, there will be more noise components in output. Secondly, often the non-time locked background EEG has larger amplitude than the time locked response. If we apply ICA to single trial EPs, the background activities components might draw more attention than the response we are interested in. Moreover, the variability in latencies and amplitudes of single trial signal may cause ICA to produce more components than what really exist [21]. Since we have limited number of sensors in EEG recording, it is preferable to focus on the time locked response than the background EEG. These reasons led us to choose average EP for the present ICA research. However, evaluation on single trial EP through ICA decomposition is a good avenue to explore.

6.2.3 Patient studies

In our study, we are limited by only a small number of patients and controls. If a larger data pool is available, we can conduct a study to compare the ICA components arising of stimulating the esophagus of patients and healthy controls

6.3 Conclusion

The results of the present research suggest that extended infomax ICA algorithm is able to separate the esophageal EP signal into components, which may have physiological origin. Present research has potential for further development. It can be easily implemented for studying patients, and perhaps serve as clinical diagnosis tool.

Chapter 7

Conclusions

Independent component analysis is a recently developed analytical procedure to study evoke potentials signal in response to electrical stimulation of esophagus. ICA decomposition may be particularly useful for comparing the latencies, time course of the signal along the afferent pathways in the brain, scalp topography and activation strength of numerous brain generators involved in producing evoked responses to a stimulus delivered to a sensory organ, peripheral nerve or a receptor.

Our studies reported in this thesis on the application of applying extended infomax ICA algorithm to averaged esophageal EP signals appear quite promising. Our results clarify and confirm the observation from earlier studies on the EP that esophageal stimulation generates cortical potentials that have several peaks each with distinct characteristics [33]. It is likely that stimulation protocols consisting of periodic and random stimulation may involve different pathways and ICA may perhaps help identify these pathways in a discriminatory fashion. Four pairs of reproducible common components were identified in response to comparing periodic stimulation and random stimulation. These four pairs of ICA components have distinctly different scalp

distributions and vary with the stimulus protocol to a large extent and with subject, and response time. The neurophysiological implication of the scalp maps as well as activation waveforms of the components, and how they related to the activity of the independent neural structures needs to be further study from both theoretical and experimental .

In addition, ICA can isolate and extract widely distributed stimulus artifact as a single output component, and remove it from the reconstructed signal.

Although the ICA technique is relatively new, and its effectiveness in separating esophageal EPs into components that reflect underlying brain processes has not yet been fully understood, the results reported here are encouraging. They demonstrate that ICA could parsimoniously decompose esophageal EP signals into temporally independent, spatially fixed, and physiologically plausible components [2]

We believe ICA may lead us to identify components of EP, which may be related to neurophysiological generators within the nervous system.

Bibliography:

1. **S. Haykin,** (editor), Unsupervised Adaptive Filtering Volume I :Blind Source Separation. *John Wiley&Sons, Inc,*2000.

2. **T.-W. Lee,** Independent Component Analysis, Theory and Applications, *Kluwer Academic Publishers,* 1998.

3. **J. Hearult, and C. Jutten,** Space or time adaptive signal processing by neural network models, *Neural Networks for Computing, AIP Conference,* 1986.

4. **P. Comon,** Independent component analysis, a new concept? *Signal Processing,* Vol.36: 287-314,1994.

5. **H. Barlow,** Sensory Communication, Possible principles underlying the transformation of sensory messages, *Guilford Publications, Incorporated,* 1961.

6. **A. Hyvarinen and E. Oja,** A fast fixed-point algorithm for independent componet analysis, *Neural Computation,* 1997.

7. **J.-F. Cardoso and B. Laheld,** Multi-channel signal separation. *In Proc. ICASSP,* 649-652, Atlanta, GA,1996.

8. **J.-F. Cardoso and S.-I. Amari,** Maximum likelihood source separation: equivariance and adaptively, *Neural Computation,* VOL. 10, PP. 251-76,1998.

9. **T.-W. Lee, A. J. Bell and R. Orglmeister,** Independent component analysis using an extended infomax algorithm for mixed subgaussian and supergaussian sources. *Neural Computation* VOL. 11: 417-41,1997.

10. **M. Gaeta and J.-L Lacoume,** Source separation without prior knowledge: the maximum likelihood solution., *Proc. EUSIPO,* 621-624,1990.

11. **J.-P. Nadal, and N. Parga,** Non linear neurons in the low noise limit: a factorial code maximizes information transfer. *Network,* 5:565-581,1994.

12. **A. Papoulis,** (editor), Probability and statistics, volumel. *Prentice Hall, New Jersey.* 1990.

13. **A. J. Bell, and I. J. Sejnowski,** An Information-Maximization Approach to Blind Separation and Blind Deconvolution. *Neural Computation* 7:1129-1159,1995.

14. **S. Amari, A. Cichochki, and H. Yang,** A New Learning Algorithm for Blind Signal Separation. *In Advances in Neural Information Processing Systems* 8:757-763,1996.

15. **S. Amari,** Natural gradient works efficiently in learning, *Neural computation* , vol 10 page 251-276,1998.

16. **M. Girolami and C. Fyfe,** Extraction of independent signal sources using a deflationary exploratory projection pursuit network with lateral inhibition. *I.E.E. Proceedings on Vision, Image and Signal Processing Journal* , 14(5):299-306,1997.

17. **A. J. Bell,** Information theory, Independent-component analysis, and applications. *Chapter, Blind Source separation,*2000.

18. **S. Makeig, A. J. Bell, T. Jung, and T. J. Sejnowski,** Independent Component Analysis of Electroencephalographic Data. *Advances in Neural Information Processing Systems* 8:145-151,1996.

19. **H. Jasper,** The 10-20 electrode system of the international Federations. *Electroenceph. Clin. Neurophysiol.* 10:370-375,1958.

20. **T. D. Lagerlund,** EEG Source Localization (Model-Dependent and Model-Independent Methods). Chapter, Electroencephalography: *Basic Principles, Clinical Applications, and Related Fields,*1995.

21. **T.-P. Jung and S. Makeig,** Independent component analysis of biomedical signals, *The 2nd Int'l Workshop on Independent Component Analysis and Signal Separation,* 633-44, 2000.

22. **S. Makeig and T.-P. Jung** , Functionally independent components of the late positive event-related potential during visual spatial attention . *JOURNAL OF NEUROSCIENCE,* VOL. 19, Page. 2665-80,1999

23. **S. Makeig and T.-P. Jung,** Independent component analysis of simulated ERP Data, *Human Higer function I: Advanced methodologies, Tnakada, Ed.* 1997.

24. **B. R. Graham** , Recording the brain's electrical activity http://core.ecu.edu/psyc.htm

25. **G. Krauthamer ,** The EEG http://www2.umdnj.edu/~neuro/neuro98/schedule/eeg_lec.htm

26. **J. P. C de Weerd and D. F. Stegeman** , Technical and methodological consideration on the measurement of evoked potentials,1988.

27. **M. V. Kamath and G. Tougas,** Estimation of habituation and signal to noise ration of cortical evoked potentials to oesophageal electrical and mechanical stimulation, *Medical and Biological Engineering and Computing,* 35:1-9,1997.

28. **T Suzuki, K Kobayashi,** Effects of stimulus repetition rate on slow and fast components of auditory brainstem responses. *Electoenceph clin Neurophysiol* 65:150-156,1986.

29. **D.G. Wastel**. Temporal uncertainty and the recovery function of the auditory EP. 1980

30. **S.Hollerbach and M.V.Kamath,** Assessment of afferent gut-brain function using cerebral evoked responses to esophageal stimulation. *Z Gastroenterology,* 36:313-324, 1998.

31. **S. Hollerbach and G. Tougas,** Cerebral Evoked Responses to Gastrointestinal stimulation in Humans, *Critical Reviews in Biomedical Engineering,* 25:203-242, 1997.

32. **S. Hollerbach and M,V. Kamath,** The cerebral response to electrical stimuli in the esophagus is altered by increasing stimulus frequencies, *Neurogastroenterology and Motility,*9:129-139,1997.

33. **G. Tougas and M,V. Kamath** , , Modulation of neurocardiac tone by esophageal stimulations in humans, *Clinical Science, 92:167-174,*1997.

34. **K. H. Chiappa,** (editor),Evoked potentials in clinical medicine, *Lippincott-Raven Publishers,*1997.

35. **R. Cooper, J.W. Osselton and J.C. Shaw,**
EEG technology.*Butterworth & Co Ltd,*1980.

36. **T. Bell ,** Basic Source separation Code ftp://ftp.cm.salk.edu/pub/tony/sep96.public

37. **A. Hyvaerinen,** Survey on independent component analysis, *Neural Computing Surveys,* vol. 2, pp. 94-128,1999.

38. **C Jutten and T. Herault,** Blind separation of sources I. An adaptive algorithm based on neuromimetic architecture, *Signal processing,* vol. 24, pp 1-10,1991.

39. **S. Haykin,** Neural Networks, a comprehensive foundation *Prentice-Hall, Inc,*1999.

40. **A. Hyvaerinen,** *1999.* Independent Component Analysis: A tutorial.
http://www.cis.hut.fi/projects/ica/

41. **S. Hollerbach and M.V. Kamath,** The Magnitude of the Central Response to Esophageal Electrical Stimulation Is Intensity Dependent, *Gastroenterology,*1997.

42. **S. Hollerbach and M.V. Kamath,** The cerebral response to electrical stimuli in the oesophagus is altered by increasing stimulus frequencies, *Gastroenterology.* 112:1137-1146,1997.

43. **Q.Frobert and A. Nielsen,** Electric stimulation of the esophageal mucosa. *Perception and brain evoked potentials,* 29,776-781,1994.

44. **T. Frieling and P Enck ,** Cerebral responses evoked by electrical stimulation of the esophagus in normal subjects, *Dig.Dis. Sci,* 34,202-205,1989.

45. **G Tougas and P Hudoba,** Cerebral evoked potential response following direct vagal and esophageal electrical stimulation in human, *Am. J. Physiol,.* 264, G486-G491,1993.

46. **T.-W. Lee and M Girolami,** A Unifying Information theoretic framework for independent component analysis, *Computers & Mathematics with Applications,* Vol 39, pp.1-21,2000.

47. **T. M. Cover and J.A. Tomas,** Elements of Information Theory. *New York Wiley,* 1995.

48. **A. Papoulis.,**Probability, Random Variables, and stochastic Process, *McGraw-Hill,* 1991.

49. **J.-F. Cardoso,** Infomax and maximum likelibhood for source separation. *IEEE letters on Signal Processing, 4:112-114,* 1997.

50. **J. Karhunen and P. Pajumen,** The nonlinear PCA criterion in blind source separation: Relations with other approaches. *Neurocomputing,* 22:5-20,1998.

51. **A. J. Bell and S. Makeig,** The `Independent Components' of natural scenes are edge filters. *Vision Research,* 1996.

52. **L. Zhukov and D. Weinstein,** Independent component analysis for EEG source localization, *IEEE Engineering in Medicine and biology Magazine.* Vol 19, Page 87-96,2000.

53. **M.V.Kamath and G. Tougas,** Estimation of habituation and signal-to-noise ratio of cortical evoked potentials to oesophageal electrical and mechanical stimulation, *Med. Biol,Eng.Comput.,* 35, 343-347,1997.

54. **T.Jung and S. Makeig,** Imaging Brain Dynamics Using Independent Component Analysis. In press, *Proceedings of the IEEE,*2001.

55. **A. Hyvaerinen and J. Karhunen,** Independent Component Analysis, *John Wiley & Sons, Inc,*2001.